

Fall 8-2012

# Development of Pesticide Sensing Polyaniline Electrode Through Detection of Alachlor By Cyclic Voltammetry

Todd M. Conner  
*University of Maine*

Follow this and additional works at: <https://digitalcommons.library.umaine.edu/honors>

 Part of the [Chemistry Commons](#)

---

## Recommended Citation

Conner, Todd M., "Development of Pesticide Sensing Polyaniline Electrode Through Detection of Alachlor By Cyclic Voltammetry" (2012). *Honors College*. 242.  
<https://digitalcommons.library.umaine.edu/honors/242>

This Honors Thesis is brought to you for free and open access by DigitalCommons@UMaine. It has been accepted for inclusion in Honors College by an authorized administrator of DigitalCommons@UMaine. For more information, please contact [um.library.technical.services@maine.edu](mailto:um.library.technical.services@maine.edu).

**DEVELOPMENT OF PESTICIDE SENSING POLYANILINE ELECTRODE THROUGH  
DETECTION OF ALACHLOR BY CYCLIC VOLTAMMETRY**

By

Todd M. Conner

A Thesis Submitted in Partial Fulfillment  
Of the Requirements for a Degree with Honors  
(in Chemistry)

The Honors College

University of Maine

August 2012

Advisory Committee:

Mitchell Bruce, Associate Professor of Chemistry, Advisor

Alice Bruce, Associate Professor of Chemistry

Scott Collins, Professor of Chemistry and LASST

Carl Tripp, Professor of Chemistry and LASST

Samuel Hanes, Fac. Associate Department of Anthropology, Honors College

## **ABSTRACT**

This research project was done to develop a chemical sensor for detection of a specific pesticide, a chlorinated herbicide called alachlor. Alachlor is an herbicide used to kill broadleaf weeds that grow mainly in corn, peanuts, and soybeans. The purpose of this project was to develop an environmentally friendly sensor in the form of an electrode that will be able to detect alachlor in aqueous samples. The way this was done was by using an electrochemical instrumentation technique called cyclic voltammetry. Polyaniline, a conducting polymer, was grown on a platinum substrate and the resulting electrode was cycled in various concentrations of alachlor in aqueous buffered samples at pH 4. By monitoring the current produced from the polymer on the metal substrate, a change in electrical current from interaction with the herbicide signaled its detection. Through additional instrumentation by SEM and FTIR it was suggested that a chemical reaction was responsible for the change in current produced by polyaniline.

## TABLE OF CONTENTS

ABSTRACT	2
LIST OF FIGURES AND TABLES	5
DEDICATION	8
Chapters	
I INTRODUCTION	9
A.) Introduction to Thesis	9
i. Description of Thesis	9
ii. Environmental Concerns of Pesticides and Alachlor	10
iii. What is a Sensor?	15
iv. Goals of Project and Thesis Statement	17
B.) Introduction to Electrochemistry	18
i. General Overview	18
ii. Experimental Techniques	21
1. Chronoamperometry	22
2. Cyclic Voltammetry	24
C.) Overview of Polyaniline	26
i. History	26
ii. Polymerization and Conductivity	28
iii. Doping Polyaniline	33
iv. Advantages and Disadvantages	36
v. Polyaniline Gas Sensing	37
D.) Overview of Scanning Electron Microscopy	38
i. Electron Microscope	39
ii. Imaging	40
E.) Overview of Diffuse Reflectance Fourier Transform Infrared Spectroscopy	42
II METHODS AND MATERIALS	44
A.) Materials and Chemicals	44
B.) Activation and Cleaning of Platinum Surface	44
C.) Polyaniline Growth	45
D.) Electrochemical Experimental Procedures	47
E.) Scanning Electron Microscopy Procedures	53
F.) Fourier Transform IR Procedures	53

III	RESULTS AND DISCUSSIONS	55
	A.) pH 5.3 Phosphate Buffer System	55
	B.) Irreversible Reduction of Polyaniline	58
	C.) Analysis of Electrical Current Trends in Polyaniline Electrode	61
	D.) SEM and FTIR Experiments	72
	E.) Reaction of Amines with Chloroacetyl Chloride	81
	F.) Interaction of Polyaniline with Alachlor	81
IV	CONCLUSIONS AND FUTURE WORK	86
	CLOSING REMARKS	89
	REFERENCES	90
	AUTHORS BIO	94

## LIST OF FIGURES AND TABLES

Figures and Tables	Page
1.1 Chemical structure of Alachlor	11
1.1 Table of Pesticide Detection Methods	14
1.2 Three-electrode cell with notations	19
1.3 Representation of reduction and oxidation processes	20
1.4 Image of a Potentiostat and diagram of Potentiostat set up with Three-electrode cell	22
1.5 (a) Plot describing step experiment. (b) Concentration profiles at various times showing decrease and increase of concentration with time (c) Corresponding current flow vs. time for b	23
1.6 (a) Current-time-potential surface for electrochemical reaction (b) Linear sweep potential across this surface	24
1.7 (a) Cyclic potential sweep (b) Resulting cyclic voltammogram	26
1.8 Chemical structure of polyaniline	26
1.9 Oxidation and reduction mechanism for polyaniline	27
1.10 Free Radical mechanism of polymerization for polyaniline	29
1.11 Cyclic voltammograms of polyaniline (HCl doped) in HCl media	30
1.12 Cyclic voltammogram of polyaniline at pH 1	31
1.13 Cyclic voltammogram of polyaniline at pH 2.5	31
1.14 Chemical structure of an 8-unit emeraldine	32
1.15 Illustration of Band Gap Principle and semiconducting materials	33
1.16 Plot of increase in conductivity of polyaniline with temperature	33

1.17	Resonance forms of emeraldine state showing ability for polyaniline to hold anions	35
1.18	Effect of TiO <sub>2</sub> on Pani/pTSA	36
1.19	Diagram showing composition of an SEM	40
1.20	Illustration showing the collection and detection of electrons in an SEM	41
1.21	Diffuse-reflectance attachment for an FTIR spectrometer utilizing an ellipsoidal mirror	43
2.1	Sample cleaning scan of platinum in 1 M H <sub>2</sub> SO <sub>4</sub>	45
2.2	Sample plot of Pani growth done to net charge of 5 C	46
2.3	Image of electrochemical cell set up for Pani growth	46
3.1	Results showing decrease in Pani signal in pH 5.3 Phosphate Buffer	56
3.2	Results of Pani cycled in low, medium, and high concentrations of ALC solution in pH 5.3 Phosphate buffer	57
3.3	Results of multiple buffer scans and ALC scan showing a decrease in Pani signal	58
3.4	Overlay showing no recovery of Pani after additional 25 cycles to fourth buffer scan	60
3.5	Results from Pani A experimental sequence	63
3.6	Plot of peak current from Pani A sequence vs. concentration of ALC	63
3.7	Results from Pani B experimental sequence	64
3.8	Plot of peak current from Pani B sequence vs. concentration of ALC	65
3.9	Results from Pani G experimental sequence	66
3.10	Plot of peak current from Pani G sequence vs. concentration of ALC	67
3.11	Average of peak currents of Pani A, Pani B, and Pani G vs. concentration of ALC	68
3.12	Peak current of Pani C through Pani F vs. concentration of ALC	68

3.13	Results of film damage test	70
3.14	Image showing a damaged and non-damaged Pani films	71
3.15	SEM image of Pani at 100 nm resolution	72
3.16	SEM image of Pani cycled with ALC at 100 nm resolution	73
3.17	SEM image of Pani at 1 $\mu$ m resolution	74
3.18	SEM image of Pani cycled with ALC at 1 $\mu$ m resolution	75
3.19	DRIFT IR spectra of Pani sample prepared 06/13/12	76
3.20	NIST FTIR spectra of Alachlor	77
3.21	DRIFT IR spectra of Pani cycled with ALC prepared 06/08/12	79
3.22	DRIFT IR spectra of Pani cycled with ALC prepared 06/13/12	79
3.23	DRIFT IR spectra of Pani cycled with ALC prepared 06/08/12	80
3.24	Synthesis of Lidocaine	81
3.25	Proposed reaction mechanism of the reduction of ALC	82
3.26	Proposed reaction mechanism of Pani with ALC	83
3.27	Diagram showing attachment active Pani chain to platinum and reaction of that chain with ALC	84



This thesis is dedicated to The Lord Jesus Christ.

The corners of each page are ascribed with AMDG, an abbreviation used for the

Ancient Christian motto:

*Ad maiorem Dei gloriam*

Translated into English as “For the greater glory of God”

This work was written *Ad maiorem Dei gloriam*.

## **CHAPTER 1: INTRODUCTION**

### **A.) Introduction to Thesis**

#### **1.) Description of Thesis**

This thesis is an outgrowth from an experience that I had in the summer of 2011 when I worked for a private company doing research with energy storage devices that encompassed using the polymer, polyaniline, as a basis for the research. I then had the idea to assimilate the things I learned and experienced on this project into what would become the basis for my senior undergraduate thesis.

In working with polyaniline, which will be described later in this chapter, I found that due to the nature of its versatility, especially on the level of conductivity, it might demonstrate the necessary qualities needed to detect something electrochemically. I wanted this project that was being created to be useful and beneficial to society in some manner. In determining what sort of species would be appropriate to use for detection I came across the water contaminant list for the U.S. environmental protection agency (EPA). The list is composed of harmful substances that are found in water by either pollution or by natural occurrence. From this list I chose the pesticide, alachlor, to which the maximum tolerance level was 0.002 mg/L. The environmental concerns of pesticides will be discussed in the next section.

I proposed to use polyaniline as a coating over a metal surface to create a basic sensing electrode. With this electrode, in an aqueous based system, I then would look for some interaction between the polymer and the pesticide that would signal a detection correlating to an actual concentration of the pesticide.

It was my theoretical idea that with time and development that this electrode would become cheap and disposable. I visualized a portable device that environmental scientists could use with this developed electrode to run controlled current experiments in the field to give quick analyses on aqueous samples; in order to avoid the time and expense of sending samples off to a lab for costly analysis. This would be a way to create a list of “hotspots” that would tell you what water sources were more concentrated than others.

However, due to time constraints this project became more of a study to show a proof of concept. The results would suggest a possible interaction between alachlor and polyaniline that could be potentially useful for the detection of alachlor in the environment. In merely just picking a pesticide and hoping for some sort of sensing interaction, I took a risk in my education and in science to reach breakthrough and success throughout the process of this project.

## 2.) Environmental Concerns of Pesticides and Alachlor

### i.) Concerns of Pesticides

Pesticides are compounds that are used to control pestilences that affect both domestic and agricultural places in society. There are many benefits to using them such as cheaper food and faster growth. However, there are many concerns that come with pesticides such as the human exposure to them. Humans can be exposed to pesticides by way of food when it is absorbed by plant roots and through accumulation on the surface of food. Humans can also be exposed to pesticides by way of water that has been contaminated. Contamination of water occurs mostly when pesticide that has been sprayed runs off into the field and then seeps into the

ground water. This run-off travels into wells, lakes, and rivers; which can be human water sources. There are also concerns with the contamination of the environment itself and not just humans by the same mechanism stated before; in addition the occurrence of drifting and leeching will affect wildlife and plant life. These factors are important motivators to develop better chemical principles and portable sensors that will be able to identify areas of contamination for treatment and avoidance.

## ii.) Alachlor

Alachlor is a type of chlorinated pesticide, more specifically an herbicide, classified as an organochlor. An herbicide is a pesticide whose primary function is to kill weeds. The molecular formula is  $C_{14}H_{20}ClNO_2$  and its chemical structure is depicted in Figure 1.1 below.

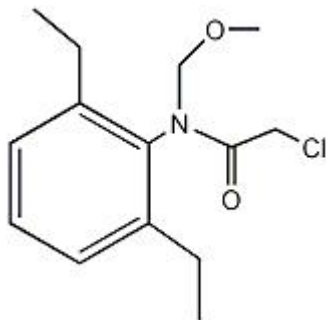


**Figure 1.1: Chemical structure of Alachlor**

Alachlor has been produced and registered by Monsanto Chemical Co. since 1969 and is used pre- or early post-emergence to control annual grasses as well as many broad-leaved weeds.<sup>2</sup> The types of crops alachlor is used to help control weeds in are maize (corn), cotton, peanuts, soybeans, and sugar cane<sup>3</sup>, all of which are heavily produced in the United States. The concerns of alachlor are that it can enter water

systems by either runoff from agricultural fields to surface water or by leaching downward into groundwater through the soil. Alachlor does not readily degrade once it reaches an aquatic system. Its tendency to leach is lessened because of biological degradation in soil, however, in areas where there is little of this and fast recharge to ground water alachlor is easily transported to ground water aquifers.<sup>2</sup> Alachlor dissipates from soil primarily by means of volatilization, photo degradation, and biodegradation.<sup>3</sup> In a phone interview with John Combest, a Monsanto communications representative, I asked him about the current sales of alachlor in the U.S. and on a global scale. He responded with a quote saying:

*“The sales of products containing alachlor are very small when compared to our company’s sales of other chemistries, particularly our branded glyphosate products.”*

Even though the production of alachlor is much smaller than it was 20 years ago, the breakdown under ground and in water is very slow. Remnants of alachlor can still be found in ground water with a maximum contaminant level of 0.002 mg/L.<sup>4</sup> This is still good cause for detection of alachlor and making sure that its contamination goes to its target level at 0 mg/L.

### iii.) Methods of Pesticide Detection

The method of detection for a pesticide is important for locating contaminated areas in the environment due to the effects of pesticides on the health of humans (food and water contamination) and the environment. Methods vary depending on the class of pesticide. Types of pesticides can be classified by the functional groups attached, such as organochlorine pesticides (OCPs),

organophosphorous pesticides (OPPs), organonitrogen pesticides (ONPs), carbamates (carbamate ester, carbamic acid group), and pyrethroids (many different functional groups). Pesticides can be classified more broadly as polar or non-polar based on their solubility in various solvents.

A pesticide detection method utilizes a chemical technique of isolation, extraction and usually pre-concentration of the pesticide before quantification via chemical instrumentation in a laboratory. The extraction part of this procedure is not necessarily done in a lab, but for more accurate results, a lab is a more appropriate environment for extraction. The method of detection varies in the detection limit for a certain pesticide. An example of this is in a study by M. Tankiewicz et al.<sup>5</sup> Various carbamates and triazines in drinking water detection limits by the field method of solid-phase extraction (SPE) were found to be between 0.1 - 0.5  $\mu\text{gL}^{-1}$ . However, for similar carbamates found in drinking water, by solid-phase micro-extraction (SPME) the detection limits were in the range of 0.6 - 19  $\mu\text{gL}^{-1}$ . This is a much higher detection limit than that of SPE. Therefore the method of detection does matter for the type of compound and the analytical study. Table 1.1 below shows a summary of current detection methods implemented for pesticides.

**Table 1.1: Pesticide Detection Methods.<sup>1</sup>**

Class	Method of Detection	Technique/Description	Lab Instrumentation	Detection Limit	
Organic Solvents	Liquid-Liquid Ext. (LLE)	Oldest and very simple. Utilizes an extraction solvent based on pesticide physical and molecular properties. (i.e. dichloromethane, pet. ether, hexane)	Vary depending on solvent, usually: GC or HPLC	Below 100 ngL <sup>-1</sup>	
	Membrane Extraction	Two classes: Membrane Assisted (MASE) and Microporous membrane (MMLLE). Both utilize a membrane that extracts the pesticide chemically.	MASE: GC-MS MMLLE: GC	1 – 10 ngL <sup>-1</sup> 1.5 – 15 ngL <sup>-1</sup>	
	Single Drop Micro Ext. (SDME)	Nearly solvent free. Utilizes transfer by using single drop of solvent. Can be done by direct immersion (DI) or by headspace (HS). Has issue of volatility with micro-droplet.	Vary depending on solvent GC or HPLC	0.21 – 0.56 ngL <sup>-1</sup>	
	Solid Phase Extraction (SPE)	Very common, uses sorption from analyte in aq. phase to a sorbent. Uses a sorbent cartridge with matrix for optimal extraction.	Vary depending on material of cartridge GC or HPLC	Example using MW Carbon Nano Tubes 2 – 3 µgL <sup>-1</sup>	
Non-Organic Solvents	Solid Phase Micro Ext. (SPME)	Eliminates org. solvents completely and is very quick. Uses adsorption of analyte onto a fibre on a micro syringe coated with an appropriate stationary phase. Uses HS or DI.	Most commonly used is GC-MS	Vary depending on material Ex. 14 – 95 ngL <sup>-1</sup>	
	Immuno-sensors: Biosensor that detects physiochemical change produced by chemical reaction in a biological interaction.	E-Chem.	Amperometric: Change in current by redox reaction. Potentiometric: Detects a potential difference in a reaction Conductimetric: Detects change in resistance in a reaction		Vary depending on IF any instrumentation is used. Most are qualitative.
		Piezo	Change in electrical signal via piezoelectric material.		
		Optical	Inhibitor reaction between target and binding analytes.		

#### iv.) Lab Instrumentation

The identification of a pesticide compound, quantification of its concentration, and the limits of detection are all determined in a controlled laboratory environment in order to obtain accurate and precise results. Results are obtained due to more suitable equipment and lower sources of error in lab rather than out in the field where there is more error.

After extraction and pre-concentration, a sample is injected into the proper instrument able to process the pesticide based on its physical properties. Most instrument techniques are chromatographic with a specific detector attached. Lab instruments used are gas chromatography (GC), which is used for compounds that are volatile and thermodynamically stable. High performance liquid chromatography (HPLC) in reversed phase mode is used for heavier compounds that usually cannot be determined by GC. Pesticides determined by HPLC are polar and thermally unstable.

The most common types of detectors that are coupled with GC are mass spectrometry (MS),<sup>6</sup> nitrogen phosphorous detector (NPD),<sup>7</sup> electron capture detector (ECD),<sup>7</sup> flame ionization detector (FID),<sup>8</sup> and thermionic specific detector (TSD).<sup>9</sup> Types of detectors coupled with HPLC are usually UV (ultraviolet light) detectors<sup>10</sup> and diode array detectors (DAD).<sup>11</sup>

#### 3.) What is a Sensor?

A sensor, specifically a chemical sensor in this case, is a device that takes chemical information, such as concentration of a specific sample or total



composition analysis of an analyte (sample component of interest) and transforms it into a signal that is analytically useful. In a broader aspect, the chemical sensor itself is the essential component of what is an analyzer. This analyzer may have devices that perform functions such as: sampling, sample transport, signal processing, and data processing.<sup>12</sup>

A chemical sensor has two basic units: a receptor and a transducer. A receptor transforms chemical information into a form of energy, which is then measured by the transducer. A transducer is a device that transforms the energy carrying the chemical information concerning the sample into an analytical signal that is useful.

The receptor piece of the chemical sensor may be based on physical, chemical or biochemical principles: physical, in which no chemical reaction takes place such as a measurement of absorbance; chemical, in which a chemical reaction with the analyte takes place to give an analytical signal; biochemical, where a biochemical process is the basis of the analytical signal such as an immunosensor. Chemical sensors are usually designed to operate under defined conditions for specific analytes in a certain type of sample so that it responds reproducibly and sensitively to the analyte of detection.

Chemical sensors are further classified by the operating principles of the transducer, including optical, electrochemical, electrical, mass sensitive, magnetic, thermometric, and other physical properties like  $\beta$ - or  $\Gamma$ - radiations. The classification for the chemical sensor in this project is an electrochemical device.

Electrochemical devices transform the effect of an electrochemical interaction of some analyte with an electrode into a useful signal. This classification can be broken into four sub-categories, which are: voltammetric sensors including amperometric devices, potentiometric sensors, chemically sensitized field effect transistors (CHEMFET), and potentiometric solid electrolyte gas sensors.<sup>12</sup> In this project, we are dealing with a voltammetric sensor as an amperometric device, in which current is measured in either the d.c. or a.c. mode. These sensors include sensors such as chemically inert electrodes, chemically active electrodes, and modified electrodes. The sensor specific to this project is a modified where the electrode itself actually participates in the interaction with the analyte.

#### 4.) Goals of Project and Thesis Statement

The following are the goals of this project:

- 1.) Show that an interaction with alachlor and the polyaniline electrode is occurring by a change in electrical current.
- 2.) Determine the trend in electrical current and analyze the signal trend to determine whether the developed polyaniline electrode is selective.
- 3.) Through instrumentation, by scanning electron microscopy and Fourier transform infrared spectroscopy, confirm that an interaction is occurring between alachlor and polyaniline and use this information to describe the interaction.

#### **Thesis Statement:**

By proof of concept, the developed electrochemical sensor described in section A.1 and in the above goals, operates to show detection of alachlor.

## **B.) Introduction to Electrochemistry**

### 1.) General Overview

Electrochemistry is a branch of chemistry that deals with the overlap of electrical and chemical effects and interactions. Much of electrochemistry deals with studying chemical changes that are caused by the passing of electrical current and production of electrical energy by chemical reactions. The field of electrochemistry is very large and encompasses many different topics such as phenomena (i.e. electrophoresis and corrosion), devices (i.e. batteries, fuel cells, and electro-analytical sensors), and technologies (i.e. the electroplating of metals for jet turbines).<sup>13</sup>

In an electrochemical system, the concerns are with processes and factors that affect the transport of charge over an interface between chemical phases (solids and liquids mainly). This is most common between an electronic conductor (e.g. an electrode, which includes solid metals like Pt and Au) and an ionic conductor (an electrolyte solution, which is a medium containing ionic species such as  $H^+$ ,  $Na^+$ , or  $Cl^-$ ). At the interface between an electrode and electrolyte solution we are concerned with the effects of when an electrical potential is applied and current is passed. Current is to be defined as the movement of electrons and holes between electrodes by the charge that is transported through the electrode. When the electrode and the electrolyte interact, this same charge passing through the electrode is then passed into the electrolyte media and carried by the movement of ions.

Experimentally, these electrochemical processes are carried out in collections of interfaces called electrochemical cells. In the case of this project we

are dealing with a three-electrode cell containing a working electrode, counter electrode, and reference electrode. A reference electrode has a fixed potential and constant makeup. The purpose of this electrode is to standardize the electrochemical cell, thus making a point of reference for any other process occurring in the cell. In this project we reference a silver-silver chloride (Ag/AgCl) electrode having a fixed potential at 0.197 V.<sup>13</sup> The arrangement below depicts this electrode.

Ag/AgCl/KCl (saturated in water)

A working electrode is the electrode of interest where a reduction and/or oxidation reaction occurs. By applying negative voltages (or potentials) to the working electrode, the energy of electrons is raised to which the level of energy will be high enough to transfer these electrons into vacant electronic states on a species within the electrolyte. This is called reduction. Similarly, applying positive potentials does the opposite, the energy of electrons will be lowered so that electrons on species in the electrolyte will favor the energy on the electrode and transfer there. This is called oxidation. Figure 1.2 depicts this process.

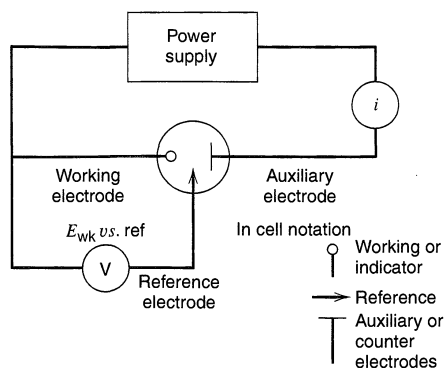


**Figure 1.2: Three-electrode cell with notations<sup>13</sup>**

A counter electrode is in a way the “receiver and passer” of current from and to the working electrode. It can be any convenient material because its properties do not affect the behavior of the working electrode. It is normally an electrode that does not produce a substance by electrolysis (chemical decomposition by electrical current) that will cause interference. Figure 1.2 represents a schematic for a three-electrode cell.

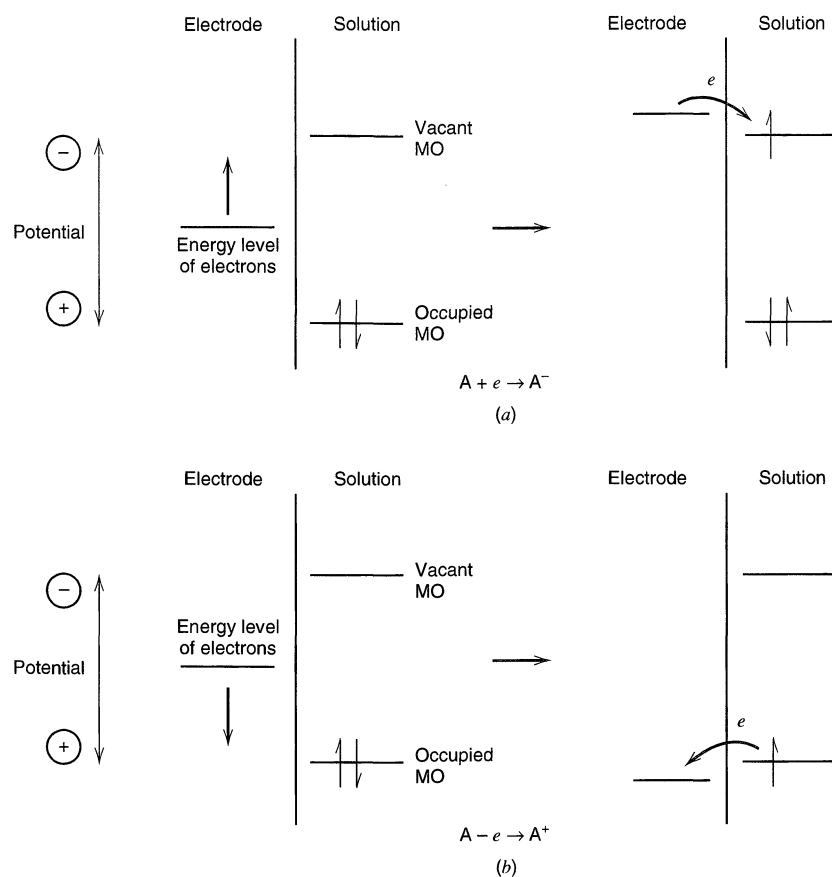


**Figure 1.3: Representation of (a) reduction and (b) oxidation processes  
MO = Molecular orbital.<sup>13</sup>**

Figure 1.3 shows a representation of reduction and oxidation processes. Part (a) of the diagram shows that when the potential is driven from positive to negative in a system, the energy of electrons is raised and vacant molecular orbitals from ionic species in solution are filled up by electrons from the electrode. Whereas in part (b), when the potential is driven from negative to positive, the energy of electrons is lowered and the occupied molecular orbitals give up electrons to the electrode.

## 2.) Experimental Techniques

This section is devoted to experimental techniques in electrochemistry that were used for this project. Experimental techniques were performed with an instrument known as a potentiostat. This instrument has control of the voltage across the working electrode-counter electrode pair, and adjusts the voltage to maintain a potential difference between the working and reference electrodes. In other words, this instrument is one whose job is to force through the working electrode whatever current is needed to achieve a desired potential at any moment.<sup>13</sup> Figure 1.4 shows an image of a potentiostat and a representation of its set up with a three-electrode cell.

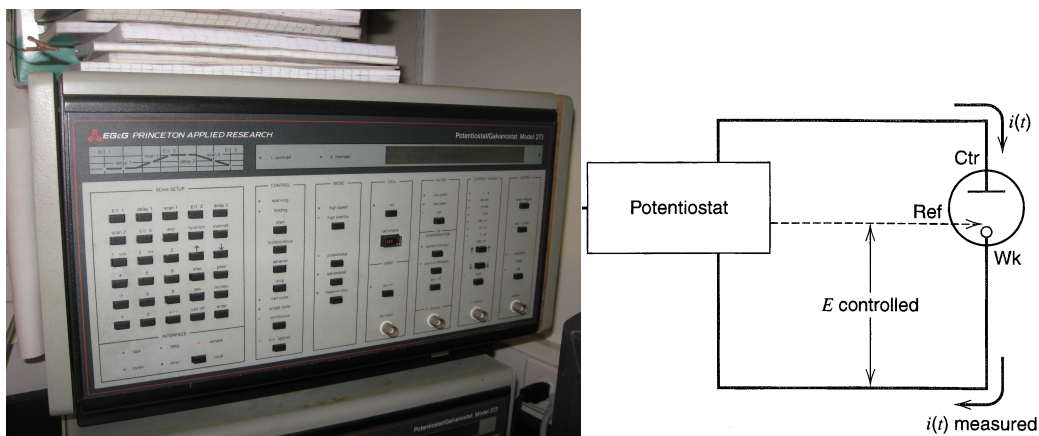


Figure 1.4: Image of a potentiostat and rep. of potentiostat set up with three-electrode cell.<sup>13</sup>

The two techniques that were mainly used in this project were chronoamperometry for polyaniline synthesis and cyclic voltammetry for experimentation in detection of the pesticide. The following are brief overviews to their set-ups and function.

#### i.) Chronoamperometry

Chronoamperometry, otherwise known as controlled potential coulometry, is the most basic of controlled potential experiments. It is the most basic because there is only one potential step. This means that the potential changes once in the time allotted for the experiment and occurs at time  $(t)=0$ . This potential is then held for the remainder of the experiment. Let  $E_1$  be the initial potential and  $E_2$  be potential after the experiment begins at  $t=0$ . For most experiments that use this technique,  $E_2$  is chosen based on the species being reacted in the electrolyte. This means that  $E_2$  is a potential that reflects the ability to reduce or oxidize a species so that it can or cannot exist at the surface of the working electrode. Due to the instantaneous

change in potential, a large current is needed to sustain reduction or oxidation at the surface of the working electrode.

The initial reduction of the species creates a concentration gradient of that species, which produces a continuing flux of that compound to the surface of the electrode for reduction or oxidation. This flux of the compound being reacted is proportional to the concentration gradient at the surface of the electrode. This means that as time goes on if the concentration at the surface of the electrode increases, the flux will increase. Thus the current is also proportional to concentration gradient because if the flux is more, then more species will be reduced or oxidized and thus increase or decrease current, depending on the species and experiment. Figure 1.5 represents the various processes occurring in a chronoamperometric experiment.

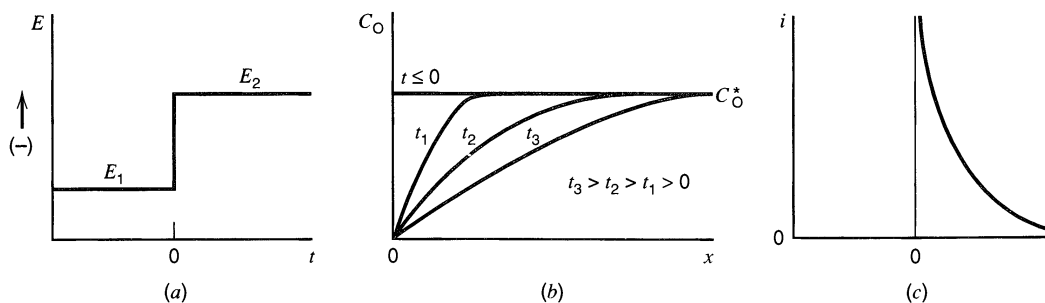


**Figure 1.5: (a) Plot describing step experiment. (b) Concentration profiles at various times showing decrease and increase of concentration with time. (c) Corresponding current flow vs. time for b.<sup>13</sup>**

In this experimental technique current is recorded as a function of time. It is also useful to record the integral of current versus time. This integral is the amount of charge passed, which is also where the term controlled potential coulometry appears. Thus a sample, like polyaniline, can be collected at the surface of platinum



at a specific potential and, as we will see later, can be collected in layers of films based on the measurement of the integral of the current passed over time and measured in coulombs (C).

## ii.) Cyclic Voltammetry

Cyclic voltammetry is a subclass of experiments known as potential sweep methods. These experiments allow for the complete electrochemical behavior of a system to be obtained through a series of steps to different potentials by recording current-time curves.<sup>13</sup> This is best illustrated as a three-dimensional current-time-potential surface, as shown in Figure 1.6.

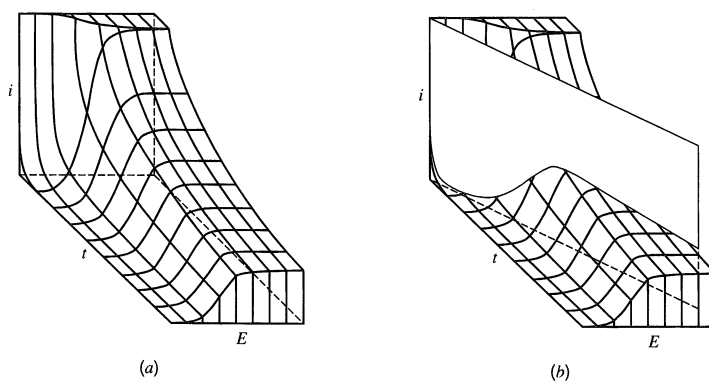


**Figure: 1.6: (a) Current-time-potential surface for electrochemical reaction. (b) Linear sweep potential across this surface.<sup>13</sup>**

The experiment is conducted by varying the potential linearly with time with a sweep rate, or a scan rate, and recording the resulting current from the system as a function of potential; this is called linear sweep voltammetry. Scan rates vary depending on the desired resolution for current versus potential in an experiment. A

slower scan rate in linear sweep voltammetry allows for a more sensitive experiment with higher resolution (low peak current), whereas a faster scan rate produces less resolution (higher peak current) and sensitivity. This interaction is due to the peak current ( $i_p$  in mA) of a reacted species being proportional to the square root of the scan rate ( $v$  in mV/s), best illustrated in Equation 1.1<sup>13</sup> for a reversible electrochemical system:

$$i_p = (2.69 \times 10^5) n^{3/2} A D_0^{1/2} C_0^* v^{1/2} \quad (1.1)$$

Scanning from a positive potential to a negative potential will result in the reduction of a species, A, and vice versa for an oxidation. The peak current is the result of a current flow that begins when the potential scan rate reaches a potential slightly positive of the reduction potential  $E^0$ . This is resultant of surface concentration being reduced at a rate that reaches a maximum at  $E^0$  and then declines, resulting in a peak current as depicted in Figure 1.7. When this potential scan reaches a specific potential and is reversed, now going in the negative to positive direction, in a reversible system (meaning the reaction will be an oxidation) the opposite will happen. This experiment is called cyclic voltammetry (CV). An example cyclic voltammogram for species A is depicted in Figure 1.7.

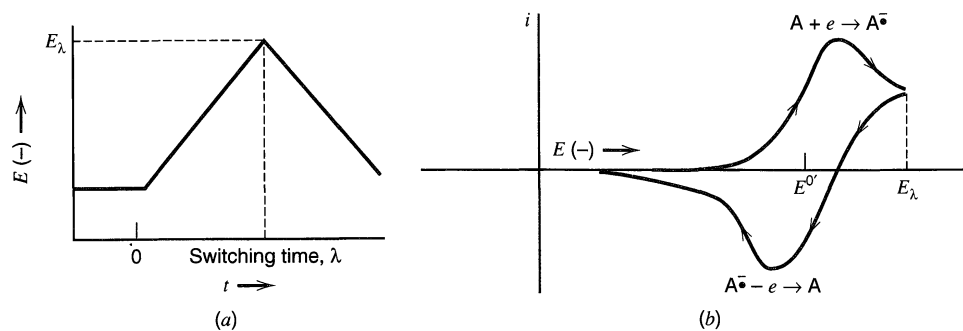


Figure 1.7: (a) Cyclic potential sweep. (b) Resulting cyclic voltammogram.<sup>13</sup>

## C.) Overview of Polyaniline

### 1.) History

The polymer polyaniline (Pani), is a semi-flexible rod polymer as well as an organic semiconductor of formula  $-(C_6H_4-NH)_n-$ , Figure 1.8 shows its structure.

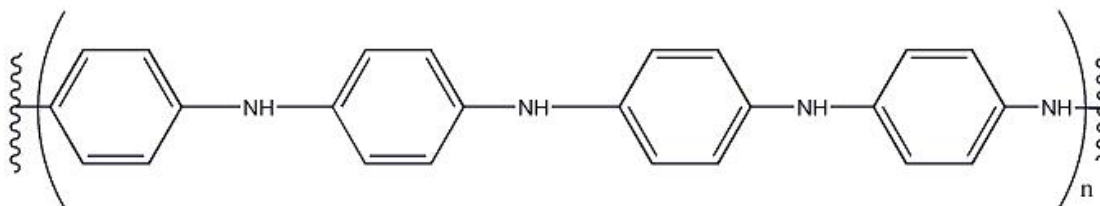
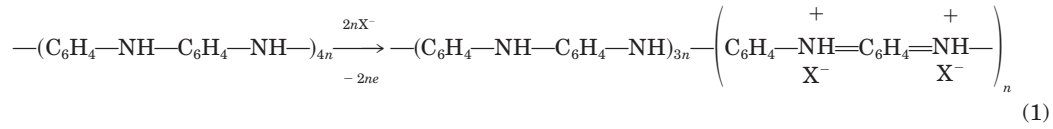


Figure 1.8: Chemical structure of Pani

The discovery of Pani dates back to Lethby in 1862.<sup>14</sup> Pani forms as a dark-green precipitate over an electrode surface when aniline is electrochemically oxidized in an aqueous sulfuric acid solution. Little further work on polyaniline was done until the 1960's when Mizoguchi and Adams developed a general mechanism for the oxidation of polyaniline, as well as general tests for ease of oxidation in acidic buffers using cyclic voltammetry.<sup>15</sup> Later, Pani was found not only to undergo polymerization when oxidized, but also to oxidize and reduce between five different

chemical states.<sup>16</sup> Figure 1.9 below shows the oxidation and reduction mechanism between states of Pani.



Leucoemeraldine (light yellow)

$\text{X}^-$  = anion as a dopant

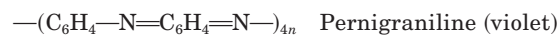
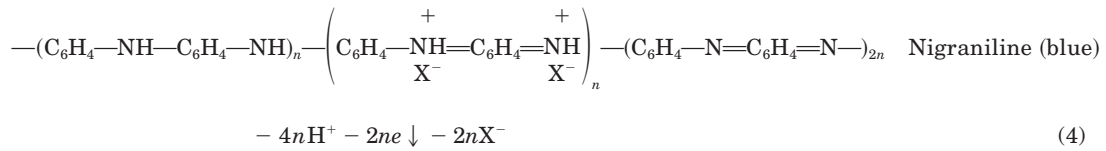
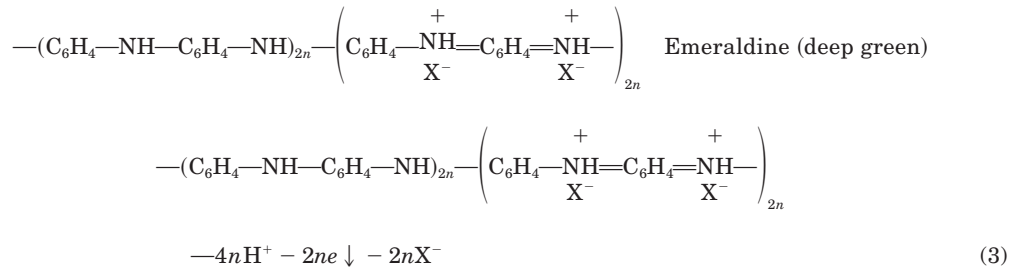
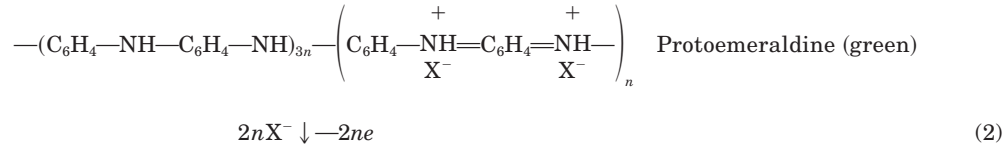


**Figure 1.9: Oxidation and Reduction mechanism for Pani.**  
Prakash et al.<sup>17</sup>

These states are distinct because they encompass a distinct color for each oxidation state, which changes when lower or higher voltage is applied: the leuco-emeraldine state, as voltage increases to oxidize the compound (when cycling potential), to the pernigraniline state. As this oxidation proceeds, the color of the solution changes from pale yellow (leuco-emeraldine) to green, then to blue, and increases to violet

as the voltage becomes more negative.<sup>18</sup> This also makes Pani its own redox indicator giving it an intrinsic property called electrochromism.

Polyaniline has been used in recent years as a membrane in gas sensing electrodes for detection of such compounds as CO<sub>2</sub>,<sup>19</sup> ammonia,<sup>20</sup> hydrogen gas,<sup>21</sup> and various toxic gases.<sup>22</sup> Pani is also used as a surface membrane for film cathodes in Li-ion polymer batteries.<sup>23</sup>

## 2.) Polymerization and Conductivity

Polymerization of polyaniline is most efficient in acidic media and is easily performed due to the low voltage required for its free radical formation. Figure 1.10 shows the proposed mechanism for the free radical polymerization of Pani. Methods of polymerization can be divided into two classes: electrochemical, using potentiodynamic (sweeping potential) or potentiostatic (constant potential) techniques;<sup>24</sup> and a precipitation method by the addition of an aniline salt dissolved into an acidic solution to yield the anilinium ion. This anilinium ion then reacts with an oxidant added, also in the form of a salt, to trigger the polymerization.<sup>25</sup> Polymerization of aniline, as stated before, yields the five chemical states of aniline where the state depends on the oxidation of the polymer.

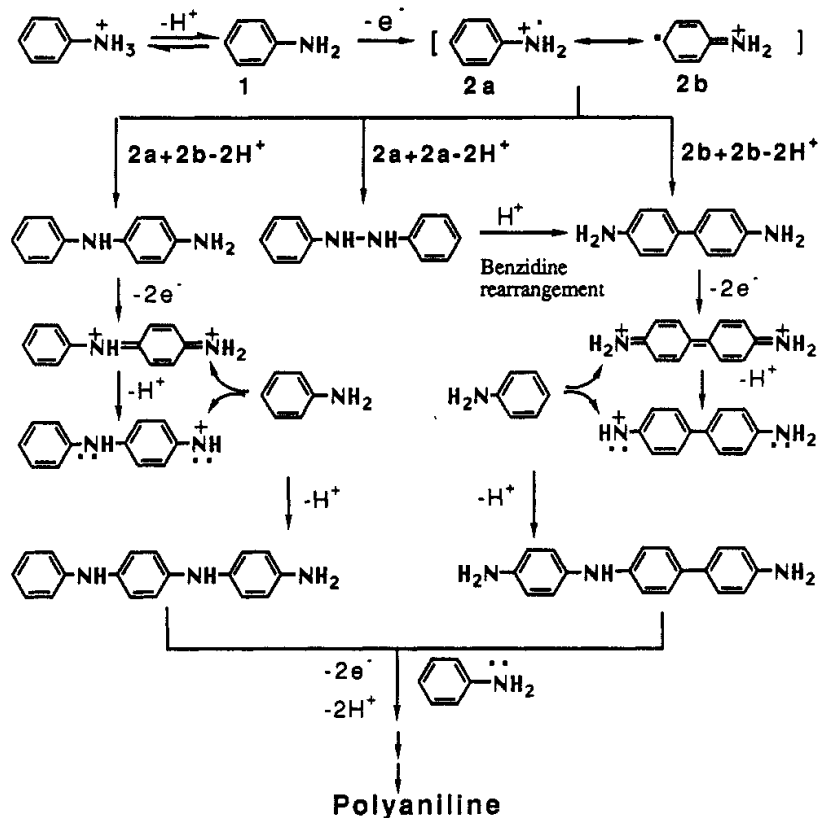
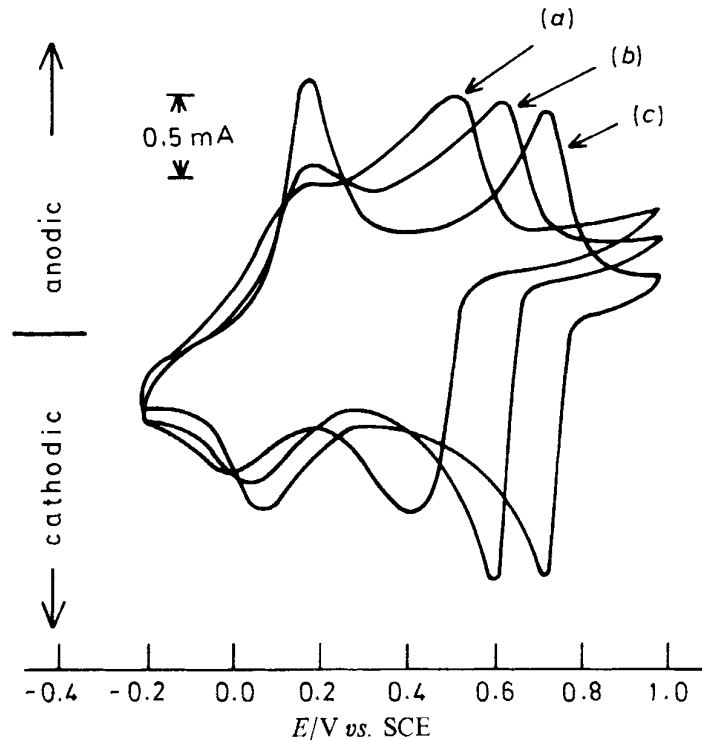


Figure 1.10: Free Radical mechanism of polymerization for Pani  
Y. Wei et al.<sup>26</sup>

On the matter of conductivity in Pani, many studies of the dependence of conductivity on oxidation state and pH have been performed.<sup>17</sup> The lower the pH, the more conductive Pani is. Figures 1.11 shows the increased conductivity (higher current) due to lower pH.

The full oxidation and reduction of Pani can be measured by a potential sweep method such as cyclic voltammetry. The states are measured this way by cycling through the redox potentials (potentiodynamic) of Pani. This potential range is between -0.2 V and +0.8 V versus saturated calomel electrode (SCE) in various acidic media such as HCl,<sup>27</sup> or H<sub>2</sub>SO<sub>4</sub>.<sup>28</sup> In this oxidation-reduction process, the number of redox peaks that can be seen depend on the media of the solution.<sup>16</sup>



**Figure 1.11: Cyclic voltammograms of Pani (HCl doped) in HCl media (a) pH 2.0, (b) pH 1.0, (c) pH 0.2. W.S. Huang et al.<sup>16</sup>**

In a low pH media like HCl, two redox peaks can typically be seen. Prakash et al. showed that these two peaks were due to the release and gain of electrons. This happens by oxidation of polyaniline first from the leuco-emeraldine state to proto-emeraldine state (Figure 1.9), then from proto-emeraldine state to emeraldine state (Figure 1.9). The counter is true for the reduction when cycling the other way through the potential range. These peaks are said to be “pH-independent” due to the fact that in their reaction mechanisms there is no proton involved in the redox reactions. Sometimes a third peak (additional gain or loss of electrons) in the voltammogram shows the pH-dependent reactions from the emeraldine state to the nigraniline state (Figure 1.9), and from there to the

pernigraniline state and vice versa (Figure 1.9). This peak in the voltammogram is broader and lower in voltage, showing the presence of protons involved in the redox reaction. However, three peaks are not always seen; Prakash et al. also showed that in a higher pH system with an acid like  $H_2SO_4$  there is a loss of conductivity to the system due to the increased pH of the system. This increase of pH reduces the ability of polyaniline to go in and out of a specific oxidation state, which can be seen through the reduced electrochromic property of the solution being cycled in.<sup>17</sup> Figures 15 and 16 show “three peak” and “two peak” voltammograms, respectively.

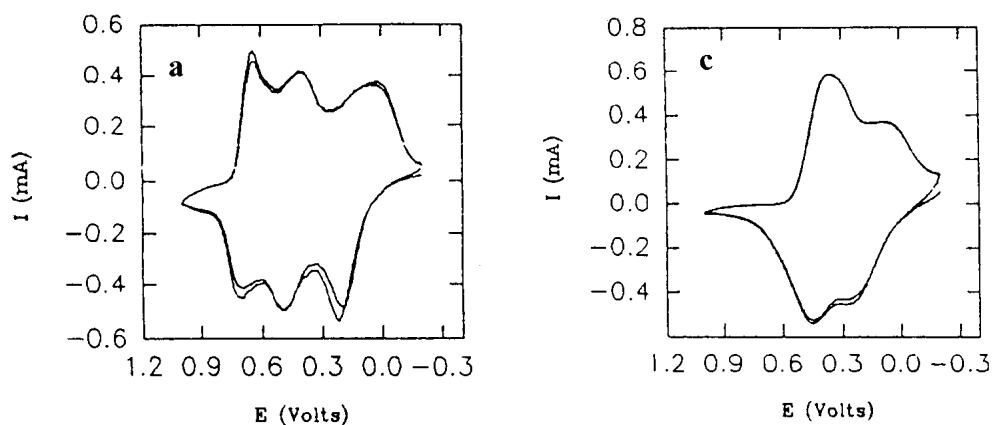


**Figure 1.12 (left) and Figure 1.13 (right): Cyclic voltammograms of Pani recorded in three-electrodes (Pt working, Pt counter, and Ag/AgCl reference). (a) pH 1.0, (c) pH 2.5. in  $H_2SO_4$  Prakash et al.<sup>17</sup>**

The conductivity of polyaniline occurs through these situations due to the oxidation of the compound to the emeraldine state, Figure 1.14 shows the chemical structure of emeraldine. In the emeraldine state the nitrogens in the oligomeric units are able resonate and form double bonds on both sides (creating a positive formal charge on the nitrogen). This forms a highly conjugated system with the



aromatic rings connecting nitrogen from one monomer to the next. As the Pani chain resonates, electrons move from the aromatic ring, to the nitrogen, to the next aromatic ring and so on. This creates a flow of electrons, which is the definition of current and thus makes Pani conductive.

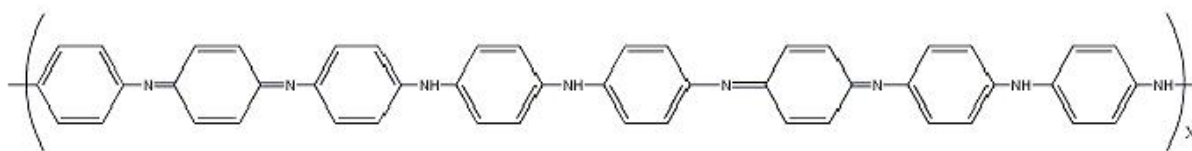


**Figure 1.14: Chemical structure of an 8 unit emeraldine.**

As stated before, Pani is an organic semiconductor (see Figure 1.16 for semiconducting trend) in pure and doped states. Pani is often doped to operate as a p-type semiconductor.<sup>29</sup> This is accredited to the highly conjugated  $\pi$ -bond system. When the polymer is thermally excited, it allows for greater delocalization of electrons and emptying of its electronic band gap (formed by the conjugated system), thus making these electrons mobile. In solid-state physics this is stated by the energy band gap principle. This principle occurs when electrons in a filled valence band are excited through a forbidden band (band gap) to the vacant conduction band, where they are then able to be mobile and thus give conductive properties to the material. Figure 1.15 shows the band scheme for a semiconductor. The largest magnitude of conductivity for Pani in its most pure form, in the most conductive state, is seen to be  $1.4 \times 10^{-8} \Omega^{-1}\text{cm}^{-1}$ .<sup>25</sup> This is not a very high conductivity value, but when additives are placed within polyaniline, the conductivity of the polymer increases dramatically and ranges between

1-10  $\Omega^{-1}\text{cm}^{-1}$ .<sup>30</sup> The conductivity in this range varies with what sort of dopant is added to Pani, this will be discussed further in the next section.

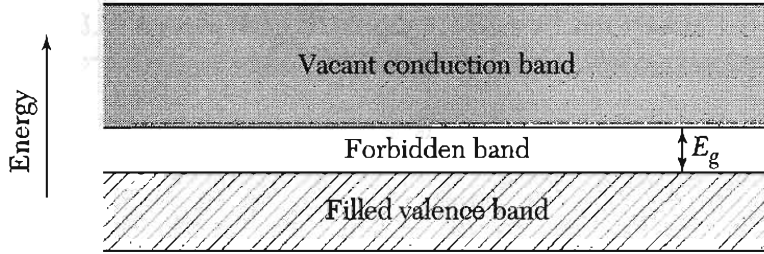


Figure 1.15: Illustration of Band Gap Principle and semiconducting materials.<sup>31</sup>

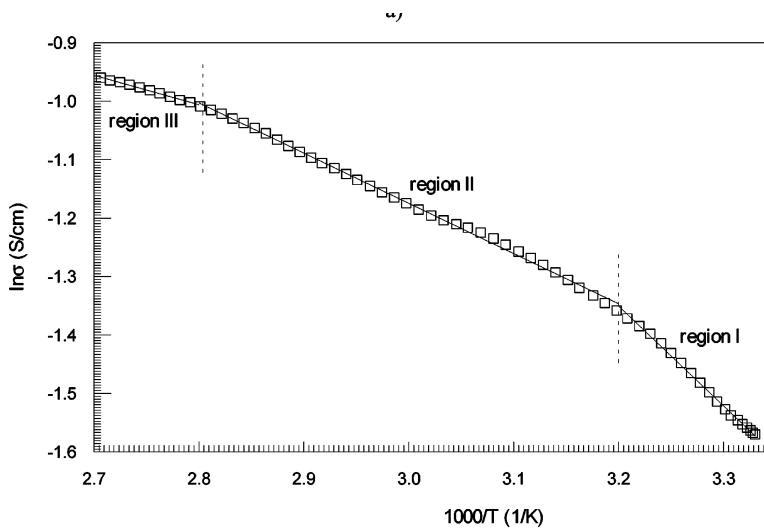


Figure 1.16: The  $\ln\sigma$  (S/cm) v.  $1000/T$  (1/K) for Pani. This shows the increase in conductivity of Pani with temperature F. Yakuphanolgu et al.<sup>32</sup>

### 3.) Doping Polyaniline

When doped Pani becomes more electrically conductive, which will vary depending on the dopant (see previous section for range of conductivity with a dopant). Doping means that impurities with specific properties are intentionally introduced into the pure compound to highlight that specific property wanted in the final product with Pani. An example of this can be seen in the work of Heera et al. by

doping Pani with PbS and CoS particles, giving the polymer an increased semiconducting property. Typical dopants for the enhancement of conductivity in Pani are camphorsulfonic acid, hydrochloric acid,<sup>33</sup> sulfuric acid,<sup>16</sup> and para-toluene sulfonic acid (pTSA).<sup>20b</sup>

The way the dopants increase the conductivity of the polymer correlates to the way the anions complex in solution with polyaniline. In the protonated state of the emeraldine form of Pani, the polymer is able to hold anions of various dopants in its “pockets” between aniline monomers. Figure 1.17 shows the structure of Pani (emeraldine state) and its ability to hold anions as well as its resonance forms.

This is able to occur due to the weak interaction from the nitrogen in the backbone of Pani. The formal charge of nitrogen is slightly positive, as shown in Figure 1.17 and is able attract and hold negative anions. When an amount of dopant that is added matches an appropriate amount of Pani, a ratio is created that creates the optimal magnitude of conductivity.<sup>33</sup>

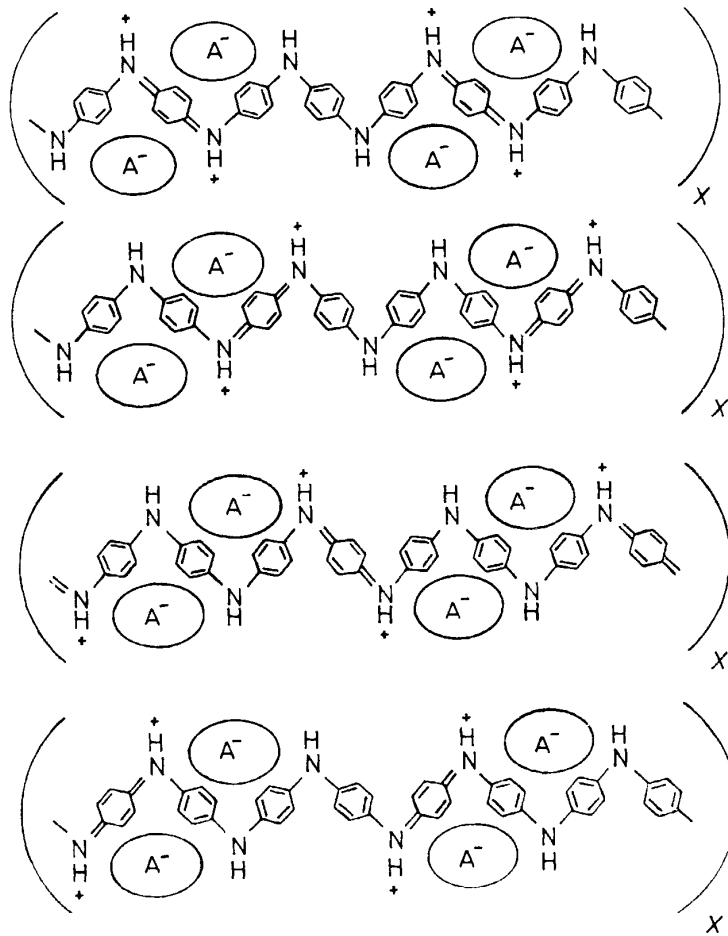


**Figure 1.17: Resonance forms of emeraldine state  
Showing ability for Pani to hold anions.  
W.S. Huang et al.<sup>16</sup>**

Metal oxides are another type of dopant that will increase the conductivity of Pani. When a metal oxide is deposited on Pani, this inorganic compound will increase the redox potential range of the polymer. This increase depends on what metal oxide is added to Pani. In the case of  $\text{TiO}_2$  and Pani, the range is increased up to 5 %.<sup>20b</sup> Figure 1.18 shows the relationship of conductivity of Pani/pTSA versus weight percent of  $\text{TiO}_2$  and Pani. This enhancement of electrochemical response can

also be seen with vanadium oxide as an example of a dopant that increases the conductivity and redox potential range of Pani.<sup>23</sup>

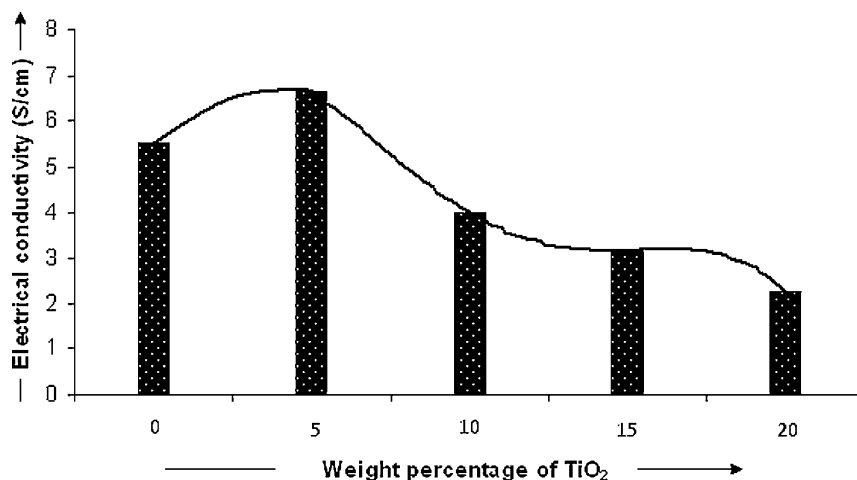


**Figure 1.18: Effect of TiO<sub>2</sub> on Pani/pTSA in a study by M.O. Ansari et al.<sup>20b</sup>  
Shows a maximum conductivity with a specific amount of TiO<sub>2</sub>**

#### 4.) Advantages and Disadvantages to Polyaniline

Polyaniline belongs to the family of organic conducting polymers that have a controllable electrical conductivity in specific acidic media and a stable chemical and electrical conductivity.<sup>17</sup> Another advantage to Pani is the resonance property of the nitrogens with the aromatic rings in the chain backbone to create a conjugated system.<sup>34</sup> This conjugated system gives polyaniline the ability to be the major component to a sensing electrode. The conjugated system becomes important upon deprotonation of the nitrogens in the backbone, this changes the form of an emeraldine salt, to an emeraldine base. This reduces the electrical conductivity because in the emeraldine base form the nitrogens are not resonating and thus the flow of electrons decreases.<sup>20b</sup>

The disadvantages to Pani with respect to its nature as a conducting polymer are that in its pure state, the polymer is sensitive to things like dissolution and in certain media may exhibit low conductivity. However, additives can be added to Pani in order to increase the conductivity as stated previously. These additives can be both organic and inorganic.<sup>20b</sup> Another disadvantage is the limited number of substrates that Pani can be deposited onto at this point in time. Pani has been deposited on metals like Au,<sup>35</sup> Pt,<sup>36</sup> Pt-coated Ti,<sup>37</sup> and stainless steel.<sup>38</sup> The majority of these metal surfaces are expensive noble metals. However, other materials that polyaniline can be deposited on are SnO<sub>2</sub>,<sup>39</sup> carbon,<sup>28</sup> and Al/C which are much cheaper substrate options for deposition.

### 5.) Polyaniline Gas Sensing

Polyaniline works as a gas-sensing polymer due to its function as an electrically conducting polymer. Polyaniline is usually coated over an electrode substrate by deposition through electrochemical polymerization. The polymerization is also usually done in the presence of a dopant (organic, inorganic, or both) in order to increase the electrical properties of polyaniline. Inorganic dopants like TiO<sub>2</sub> are often used in polyaniline due to its unique dielectric constant and large energy gap.<sup>21</sup> Organic acids are also good choices because of their nature to lower the pH of polyaniline, creating a more conductive environment for polyaniline. Organic acids like p-toluenesulfonic acid are often used.<sup>20b</sup>

Polyaniline undergoes a change in electrical resistance when exposed to a vapor. This is due to the interaction of the vapor with the emeraldine salt. When a

salt is reformed as the emeraldine base, the conductivity of polyaniline is reduced. Studies show detection of vapor by polyaniline for gases like ammonia (NH<sub>3</sub>),<sup>20b</sup> carbon dioxide (CO<sub>2</sub>),<sup>19</sup> hydrogen (H<sub>2</sub>),<sup>21</sup> and various other toxic gases.<sup>22</sup>

Polyaniline nanocomposites have also been used in most recent endeavors to detect vapors by the change in electrical resistance. However these nanocomposites reside in solution and not on a specific electrode substrate.<sup>20b</sup>

Polyaniline also is used as an electrically conductive sensor for some types of liquids, like alcohols (methanol, ethanol, and 1-propanol).<sup>40</sup> This sensor exhibits sensitivity to the different alcohols showing higher increase in resistance upon exposure with the larger alcohol (1-propanol), and a lower increase with the smallest (methanol). This sensor is based on ternary immiscible polymer blends and works on the same principle as the gas sensor in detection and measurement of an analyte by a change in electrical resistance.

#### **D.) Overview of Scanning Electron Microscopy (SEM)**

Scanning electron microscopy (SEM, same abbreviation for microscope) is an imaging technique that uses an electron microscope and electrons to image a sample. These electrons that are used to image a sample interact with the atoms of the sample in a way to image the surface topography of the sample, the composition, as well as other properties such as electrical conductivity.

Historically, the first SEM image was obtained by Max Knoll in 1935 when he was able to image silicon steel and its electron channeling differences.<sup>41</sup> The SEM was developed into a commercial instrument by Sir Charles Oatley and his

postgraduate student Gary Stewart and was first commercialized in 1965 by the Cambridge Scientific Instrument Company as the “Stereoscan”.<sup>42</sup> The first of these instruments was delivered to DuPont.

### 1.) Electron Microscope Overview

The SEM is composed in the same fashion as a common microscope used for biological study. However instead of using a light source like a common microscope uses, an electron source is used. This is called an electron gun. In a typical SEM the electron gun emits an electron beam thermionically (using heat). The gun usually utilizes a tungsten filament cathode due to its high melting point, low cost, very low vapor pressure. However, many other types of materials are used for the electron gun such as lanthanum hexaboride ( $\text{LaB}_6$ ). This electron beam can have energy anywhere on the magnitude of 0.4 keV to 40 keV. This beam passes through a pair of condenser lenses that focus the beam to a small spot (between 0.4 nm and 5 nm). The beam then passes through a third lens, an objective lens which consists of scanning coils that deflect the beam in an x and y axis pattern so that it will scan in a rastered (rectangular) manner. Magnification of the sample is controlled by the voltage that is supplied to these x and y coils. A schematic diagram is depicted below in Figure 1.19 to show the composition of an SEM.



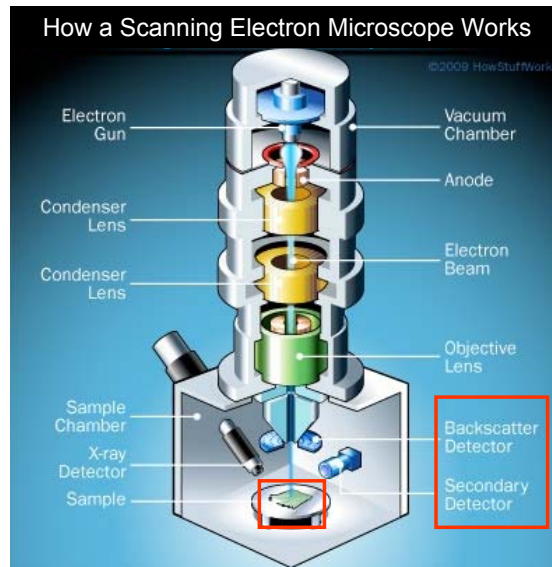


**Figure 1.19: Diagram showing composition of an SEM (Diagram courtesy of Prof. Scott D. Collins)**

## 2.) Imaging

SEM images with what are known as secondary electrons and backscattered electrons. However, characteristic X-rays and light (cathodoluminescence) are often used as well to image a sample. Secondary electrons are generated by the ionization of a sample as a result of the interactions of the electron beam either on the sample or near it (a few nanometers). The resolution of an image using these types of electrons is  $\sim 1$  nm. These electrons utilize a Everhart-Thornley detector,<sup>43</sup> consisting of a Faraday cage in conjunction with a scintillator and a photomultiplier tube. The Faraday cage attracts the electrons from the surface with a low positive voltage and the scintillator takes these electrons and accelerates them with a higher positive voltage as to produce light photons. This is channeled to the photomultiplier tube, which in turn amplifies this electron signal to the computer for imaging. A secondary electron detector is positioned usually a little off to the side of the sample because the intensity of electrons will increase with the increase

of the angle of incidence. An illustration in Figure 1.20 shows how electrons are detected in a typical SEM.

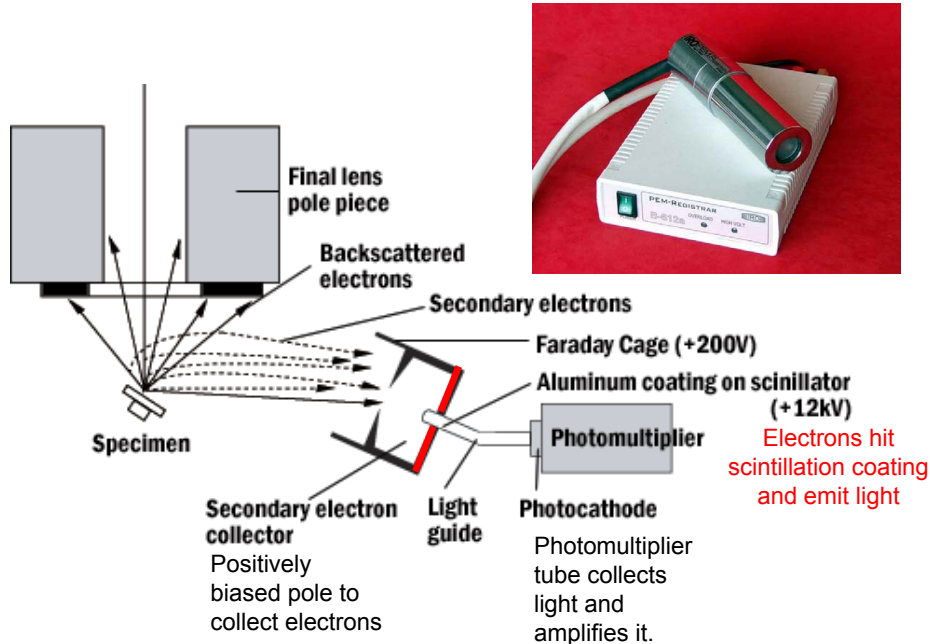


**Figure 1.20: Illustration showing the collection and detection of electrons in an SEM (Image courtesy of Prof. Scott Collins)**

Backscattered electrons (BSEs) are high-energy electrons that are the resultant of elastic scattering interactions with the sample atoms. Heavier elements with higher atomic number backscatter electrons much better than light, low atomic number elements. This allows the ability to show the contrast between different chemical compositions using BSEs. BSE detectors are placed above the sample around the electron beam unlike the Everhart-Thornley detectors placed on the side. This is because the high-energy BSEs are found to be more concentric with the electron beam. BSE detectors are usually of the scintillator nature, but semiconductor devices can also be used to obtain signals from BSEs.

Specimens that are non-conducting usually need to be coated in a conducting material such as a metal. Metals that are often used are gold, palladium, platinum, palladium/gold alloy, tungsten, and graphite. Conducting materials need not be coated in anything for imaging.

### **E.) Overview of Diffuse Reflectance Infrared Fourier Transform Spectroscopy**

Diffuse reflectance spectroscopy (DRIFT) is a highly sensitive technique for obtaining infrared spectra on a powdered sample or a sample with a rough surface. It requires minimal sample preparation and does not affect the chemical or physical properties of the sample. Samples are usually ground and mixed in with KBr or KCl (both are IR inactive). DRIFT is a highly sensitive technique that encompasses a complex process. Diffuse reflectance occurs when a beam of radiation strikes the surface of the fine powder, or rough sample. This causes specular reflection at each plane surface, which then causes radiation reflection in all directions, due to the presence of many surfaces. Even though this is a reflection technique, absorbance is still a factor in this process where the reflected beam hits the sample and the sample absorbs the radiation. After the radiation is absorbed, some is then reflected back to the detector. The most widely used model to represent this was developed by Kubelka and Munk,<sup>44</sup> where equation 1.5 and 1.6 were developed to show relative reflectance intensity for a powder's  $f(R)$ , where  $R$  is the ratio of reflected intensity and  $k$  is the molar absorption coefficient of the analyte.

$$f(R'_\infty) = \frac{(1 - R'_\infty)^2}{2R'_\infty} = \frac{k}{s} \quad (1.5)$$

$$k = 2.303\epsilon c \quad (1.6)$$

Equation 1.6 shows a proportional relationship, like that of the Beers-Lambert law, of absorbance to concentration taking into account the reflectance off the surface of the sample. A specialized attachment is required to obtain DRIFT spectra in which the collimated beam of radiation from the interferometer is directed to an ellipsoidal mirror and then to the sample. Figure 1.24 shows a diagram for common diffuse reflectance attachment for an FTIR spectrometer.

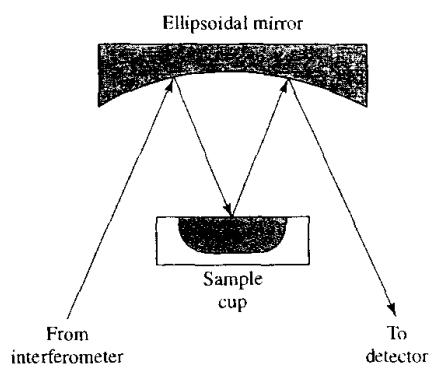


**Figure 1.21: Diffuse-reflectance attachment for an FTIR spectrometer utilizing an ellipsoidal mirror.<sup>45</sup>**

## **CHAPTER 2: Methods and Materials**

### **A.) Materials and Chemicals**

All aniline was purchased from Sigma-Aldrich as ACS reagent grade and then double distilled. All alachlor (abbreviated ALC) was purchased from Sigma-Aldrich as PESTANAL<sup>®</sup>, analytical standard grade. All aqueous based solutions were made using deionized water (HPLC grade) purchased from Fisher Scientific. All electrolytes used, with the exception of tetrabutylammonium chloride hydrate, were of anhydrous grade. All electrochemical experiments were conducted by using a Princeton Applied Research (PAR) potentiostat 273A. SEM was done using a Zeiss N-Vision 40 electron microscope. IR spectroscopy was done using an ABB-Bomem FT/LA Spectrometer and a Herrick Preying Mantis DRIFT attachment.

### **B.) Activation and Cleaning of Platinum Surface**

Activation and cleaning experiments were implemented each time before conducting polyaniline synthesis on the surface of platinum electrodes. These experiments were conducted once by cycling a piece of bare platinum foil, as the working electrode, in 1 M H<sub>2</sub>SO<sub>4</sub> solution between 0 V and 1.2 V at 125 mV/s for 20 cycles.<sup>46</sup> A platinum wire was implemented as a counter electrode and Ag/AgCl electrode as the reference. This experiment was done so that any impurities that may have been residing on the surface were cleaned off before synthesis. Figure 2.1 below depicts the last (20<sup>th</sup>) and second to last (19<sup>th</sup>) scans in a cleaning procedure done before an experiment.

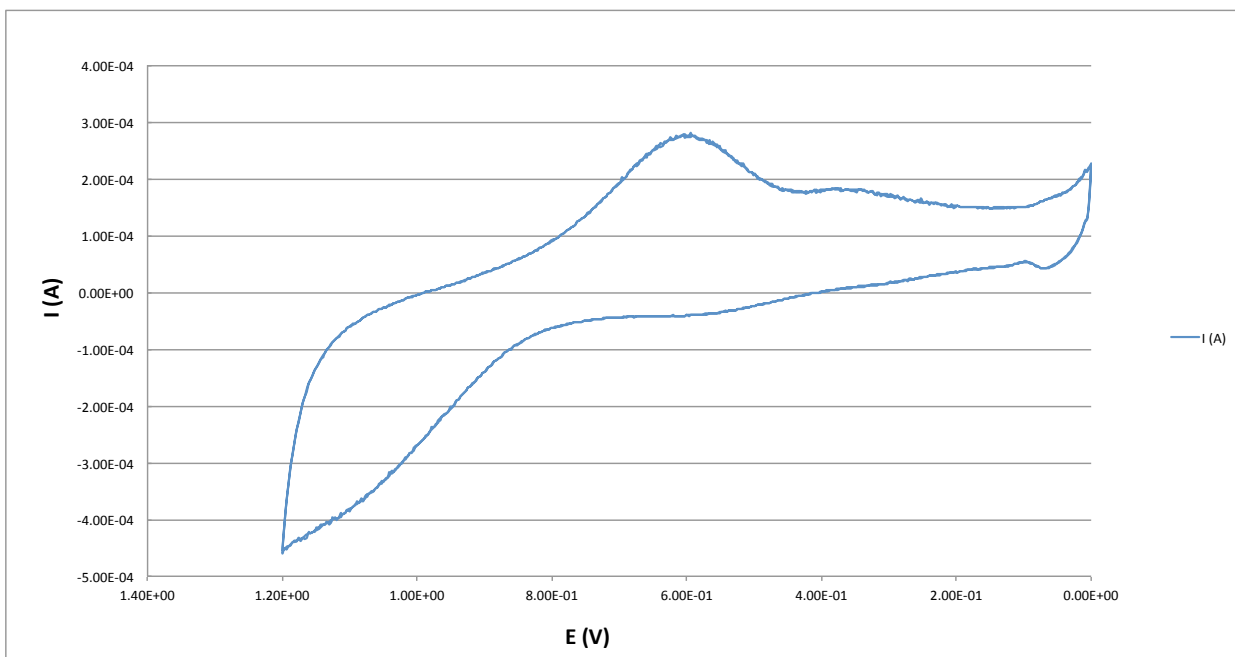


**Figure 2.1: Sample cleaning scan of platinum in 1 M H<sub>2</sub>SO<sub>4</sub>**

### **C.) Polyaniline (Pani) Film Growth**

Polyaniline films were synthesized from 0.40 M aniline growth solution in HPLC grade H<sub>2</sub>O. This solution was adjusted to pH 1.3 by a 1 M H<sub>2</sub>SO<sub>4</sub> solution. This adjustment to pH 1.3 was done to optimize the growth of polyaniline due to the increase in conductivity of polyaniline at a lower pH. All growths were done electrostatically in a single cell at 0.825 V. The growth was done over a piece of platinum foil as the working electrode for growth, unless indicated in the following electrochemical experimental sections. The counter electrode used was a double Ni electrode placed on each side of the platinum electrode in the cell, linked by a lead (as shown in Figure 2.2 below). The amount of polyaniline grown for each experiment varied on what experimental procedure was being employed. The amount of polyaniline that was grown over platinum substrate was measured by

charge in units of Coulombs (C). Figure 2.3 below depicts the growth over time in current being generated by Pani as it grows over the platinum at 0.825 V.

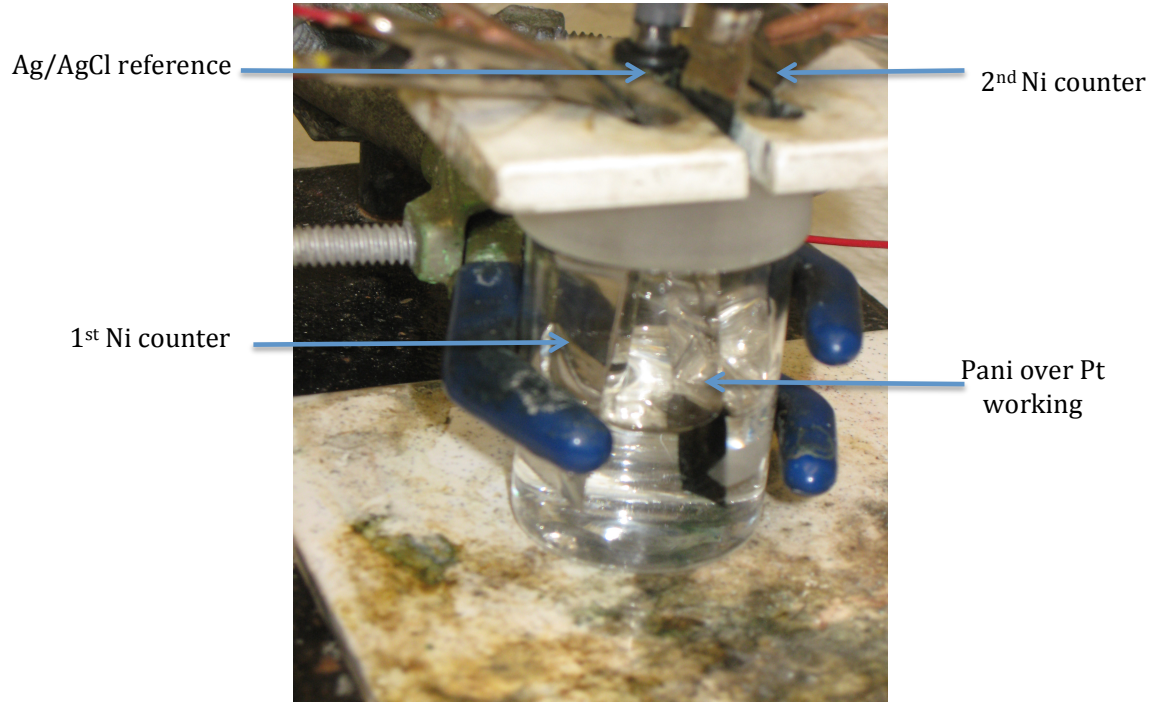


Figure 2.2: Image of electrochemical cell set up for Pani growth

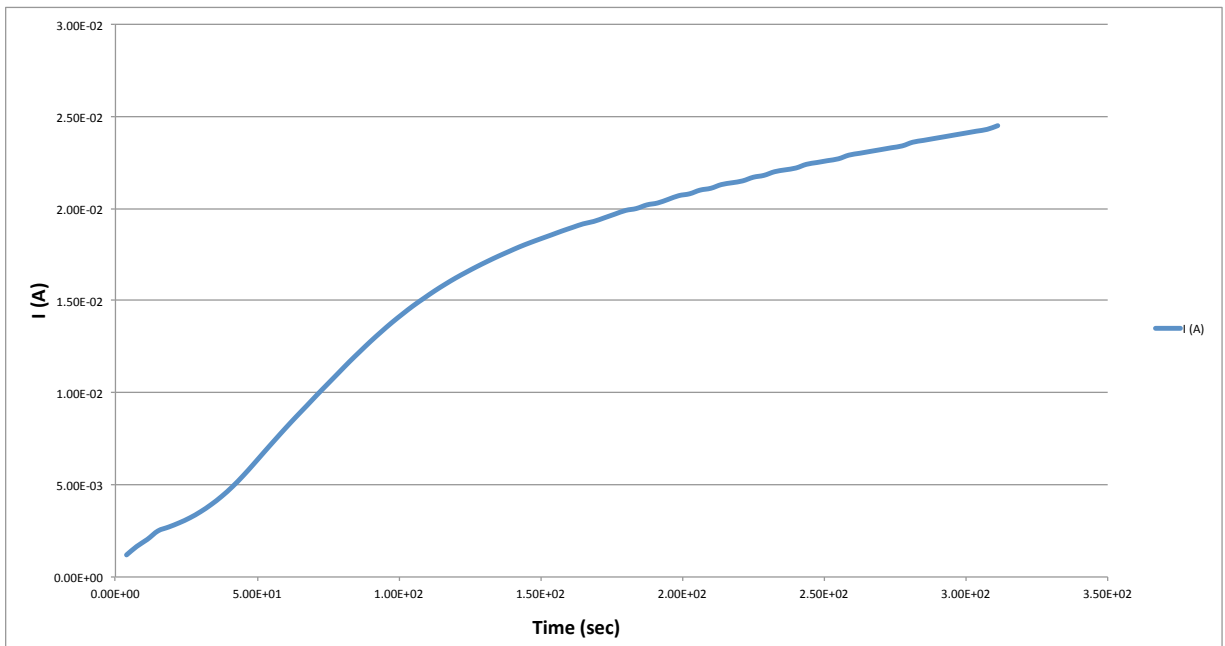


Figure 2.3: Sample plot of Pani growth done to net charge of 5 C

## **D.) Electrochemical Experimental Procedures**

The following covers the experimental systems that were developed over the course of this project in order to reach the point of a simple, working pesticide sensor. The system is defined as the liquid media in which electrochemical experiments were conducted in, as well as the way in which alachlor was placed in solution and added to the liquid media for experiments. Each system developed was a step in the incremental development of the final system implemented for the basic workings of the pesticide sensor. All experiments were done at room temperature (~20 °C).

### **i.) Aqueous KCl Solutions**

Aqueous solutions of 0.2 M KCl (for electrolyte) were made to start as the media for experimentation. These solutions were made with HPLC grade H<sub>2</sub>O and were adjusted to pH 2 and pH 1.3 by 0.2 M HCl and 0.2 M NaOH. Alachlor was dissolved in Methanol (MeOH) in various concentrations and added during scans to simply see what it would do to the current signal. These experiments varied in the way they were conducted in order to be able to try and see what kind of result each procedure would give. The first media used was a pH 2 KCl solution, which later was lowered to pH 1.3. Polyaniline was grown over platinum to 10 C. The solution was cycled between +1.0 V and -1.0 V for 3 cycles each experiment while ALC in MeOH was added incrementally to see a change in current from the working electrode. Various scan rates were implemented from slower (10 mV/s) to faster (100 mV/s)



to simply see what sort of signal was produced. An Ag/AgCl reference electrode was used for all experiments, as well as platinum wire as a counter.

It was seen that when the KCl media was used to cycle Pani, the signal showed distinct redox peaks for the Pani baseline signal, however, when ALC in MeOH was added during a scan, the current signal would dramatically decrease the signal of the polymer and give off a lot of noise. It was seen that MeOH might not be a good solvent choice, as well that the KCl solution may not have been the best choice either for experimental solution. This lead to the next implemented experimental procedure.

#### ii.) pH 2.5 H<sub>2</sub>O by H<sub>2</sub>SO<sub>4</sub> Solutions

After the finding of the results from the previous system, a different experimental solution was investigated in order to gain better compatibility with the addition of ALC in MeOH (various concentrations). Therefore a simple aqueous solution was made at pH 2.5 by addition of H<sub>2</sub>SO<sub>4</sub> for pH adjustment and electrolyte. pH 2.5 was implemented to begin an attempt to increase pH due to the better reactivity of ALC under basic conditions. However, the extremely acidic pH system was used to start with in order to obtain a strong Pani signal that would show an effect when exposed to ALC. Bare platinum was cycled between +1.4 and -1.3 V for 3 cycles in this solution in order to see if when ALC was added it would reduce at the surface platinum the way that ALC reduced at HMDE by El-Shawahi et al. As well, other ALC solvents were used to see what sorts of current responses could be generated in this system. An Ag/AgCl reference was used for all experiments as well as a platinum wire for counter and the system aerated with N<sub>2</sub>.

Pani was not used as the working electrode in any of these experiments because the idea behind implementing this system was to study the interactions between experimental solutions and the addition of ALC, as well whether an actual reduction of the pesticide could be seen electrochemically. The reduction of ALC was unable to be seen where expected (around -1.3 V) at the surface of platinum in this system due to electrolysis of water that occurs around -1.0 V.

MeOH was seen to be a solvent that when added to the aqueous experimental solution had very poor electrical conductivity and reduced the current greatly. Other solvents were used for dissolving ALC such as propylene carbonate (PC) and acetonitrile (ACN). These solvents turned out to also decrease the conductivity of the aqueous experimental solution when added during cycling.

These investigations led to implementing a non-aqueous experimental solution that would be the same as that of what ALC was dissolved in and then added during a scan since it was seen that conductivity decreased dramatically when a non-aqueous solvent was added to an experimental aqueous solution.

### iii.) Non-Aqueous Acetonitrile Solutions

Solutions of 0.1 M Tetrabutylammonium chloride hydrate (TBACH) in acetonitrile (ACN) were made for experimental media. Various concentrations on the mM level of ALC in ACN were made using this experimental media. Experiments were done at various scan rates between 10 mV/s and 150 mV/s and cycled from +1.0 V to -1.5 V for 3 cycles. Pani was grown to ~2 C. An SCE reference electrode was used for all non-aqueous experiments as well as platinum wire for a counter and the system aerated with N<sub>2</sub>.

Non-aqueous solutions were investigated as electrochemical media for experiments after the low pH water by H<sub>2</sub>SO<sub>4</sub> for a few various reasons. The first was done in order to see if the herbicide could directly be reduced at the surface of bare platinum, with no polyaniline and without electrolysis of water inhibiting the ability to see an irreversible reduction peak around -1.3 V. This would give evidence to support a primary way of sensing the herbicide by measuring actual current given by the reduction of ALC. The second reason was if I could see an irreversible reduction peak on bare platinum, then it would be possible to coat polyaniline over platinum and cycle the electrode in non-aqueous to provide the means for seeing the reduction of ALC. This reduction would hopefully show either an increase or decrease in conductivity of polyaniline for a secondary means of detection.

After the development of this reasoning, it was found that reduction of ALC could not be seen at the surface of bare platinum in non-aqueous media. After further literature investigation it was seen that El-Shawahi et al. was able to reduce ALC directly at the surface of HMDE by using a cathodic stripping voltammetry technique, which utilizes identifying a specific ionic species of the herbicide by collecting or electroplating the herbicide at the surface of a working electrode and then reducing it from the surface by stripping it off. The electroplating step is accomplished by holding the electrode at an oxidizing potential and the stripping by sweeping the potential positively. This technique was found to not be beneficial to this project and its cause for an environmentally safe sensor, as it uses a mercury film as the basis for plating.

Pani experiments in non-aqueous media also were seen to produce poor current response even in a background and thus no conclusion about Pani cycled with ALC could be drawn in non-aqueous media except to return to investigating the an aqueous based system.

#### iv.) Phosphate Buffer Solutions

0.1 M Phosphate buffer solutions at pH 5.3 were made using 1 M solutions of potassium phosphate dibasic ( $K_2HPO_4$ ) and potassium phosphate monobasic ( $KH_2PO_4$ ). As well ALC was discovered, by a study done by Carrai et al.,<sup>47</sup> to be able to be put indirectly into aqueous media by dissolving ALC in acetone and then mixing ALC in acetone with a phosphate buffer solution. Therefore, 0.500 g of ALC were dissolved in 10 mL of acetone yielding a  $1.853 \times 10^{-1}$  M solution of ALC; 1 mL of this solution was taken and dissolved in 250 mL of phosphate buffer yielding a  $7.414 \times 10^{-4}$  M ALC solution in phosphate buffer. This then became the stock solution. Successive dilutions were then made in 1/2, 1/4, 1/8, and 1/16 increments from the stock. Pani was grown to  $\sim 2$  C for all experiments. Experiments were carried out from 0.825 V to -1.5 V for varying cycle amounts. The scan rate for all experiments was done at 10 mV/s. For all experiments, an Ag/AgCl reference electrode was used, platinum wire as the counter, the system was aerated with  $N_2$ , and for the working electrode a homemade 1 mm platinum wire encased in glass tubing was used.

#### v.) Aqueous Universal Buffer Solutions

A universal buffer mixture at pH 4 was created using McIlvaine's buffer using a 0.1 M citric acid solution and a 0.2 M sodium phosphate dibasic solution.<sup>48</sup> This pH 4 buffer solution was then used to make a  $7.414 \times 10^{-4}$  M ALC stock solution in the same manner as described in the previous section. Three successive dilutions of  $4.634 \times 10^{-5}$  M,  $1.158 \times 10^{-5}$  M, and  $2.895 \times 10^{-6}$  M were prepared to obtain the three minimal concentration points needed to create a calibration curve for this sensor. Electrochemical experiments were done first by cleaning the bare platinum electrode, a piece of platinum foil that utilized  $\sim 1$  cm<sup>2</sup> working electrode area. The platinum electrode was then placed in the aniline growth solution and grown to  $\sim 5$  C. All experiments, unless indicated, in this system consisted of running a Pani electrode background in just pH 4 buffer, then cycling the Pani electrode in the  $2.895 \times 10^{-6}$  M ALC solution, then cycling the Pani electrode in  $1.158 \times 10^{-5}$  M ALC solution, and then finally cycling in the  $4.634 \times 10^{-5}$  M ALC solution. Experiments were done for 3 cycles from +0.825 V to -1.5 V at a rate of 10 mV/s.

In order to analyze the interaction Pani was having with ALC, a special experimental sequence was conducted. This sequence utilized a homemade platinum electrode with a 1 mm platinum wire encased in glass. The platinum electrode was placed in aniline solution and Pani was grown to  $\sim 100$  mC. Then the Pani electrode was scanned for 1 cycle in pH 4 buffer from +0.825 V to -1.5 V at a scan rate of 10 mV/s. A second buffer scan was then done under these same conditions. Then, another scan was done in a  $2.895 \times 10^{-6}$  M ALC solution for 1 cycle under the same parameters. Afterwards, a third buffer scan was done for a single

cycle under the same parameter, and then a fourth buffer scan was done under these same conditions. Afterwards, a buffer scan was done in the same voltage range at the same scan rate for 25 cycles. A platinum wire was used as a counter and an Ag/AgCl electrode as a reference for all experiments. All experiments were done in a single cell and aerated with N<sub>2</sub>.

### **E.) Scanning Electron Microscopy (SEM) Experimental Procedures**

SEM was used in order to evaluate a sample of Pani cycled in just pH 4 buffer versus a sample of Pani that was cycled in pH 4 buffer, then cycled in  $2.895 \times 10^{-6}$  M ALC solution, then  $1.158 \times 10^{-5}$  M ALC solution, then  $4.634 \times 10^{-5}$  M solution, and then finally in  $7.414 \times 10^{-4}$  M ALC solution. All electrochemical experiments were done under the same conditions as described in the Aqueous Universal Buffer section. These two films were dried under N<sub>2</sub> in an IR oven at 300 °C for 20 minutes each. Detectors used for image capture were SE2 and InLens. A single detector was used for each image. The system vacuum varied around the level of  $1 \times 10^{-6}$  Torr. The electron beam voltage used for the majority of the images was 10 kV. Images were taken at various resolutions and for this study resolutions of 1 μm and 100 nm were investigated.

### **F.) DRIFT Spectroscopy**

FTIR was used in order to evaluate the bond makeup of a sample of Pani cycled in just pH 4 buffer and three samples of Pani cycled in pH 4 buffer, followed by being cycled in  $2.895 \times 10^{-6}$  M ALC solution, then  $1.158 \times 10^{-5}$  M ALC solution,

then  $4.634 \times 10^{-5}$  M solution, and then finally in  $7.414 \times 10^{-4}$  M ALC solution. All electrochemical experiments were done under the same conditions as described in the Aqueous Universal Buffer section with the addition of scraping each film after drying and crushing to refine the fibers as much to powder as possible. The scan collection for each spectra was 500. A DRIFT reflection technique was used in order to evaluate the samples.

## **CHAPTER 3: RESULTS AND DISCUSSIONS**

The discussion is based on data that was collected from using the pH 5.3 phosphate buffer and pH 4 aqueous universal buffer systems. All other systems data up until the point of implementing these systems were discussed in the methods sections and found to be helpful in the development of a working system for the pesticide-sensing electrode.

### **A.) pH 5.3 Phosphate Buffer System**

This particular system was the first that began to provide significant data that suggested something was happening between Pani and ALC. Figure 3.1 is an overlay of cyclic voltammograms that show when ALC is cycled in solution with Pani, the signal is decreased dramatically. The baseline Pani scan, outlined in red, shows that there is a distinct redox couple for Pani in the pH 5.3 phosphate buffer. However, when the Pani electrode is cycled in ALC solution, the current signal shrinks and the oxidation peak actually disappears. As will be discussed later, this gave the first hint that an actual irreversible reaction may be occurring between Pani and ALC after the reduction of ALC in solution.



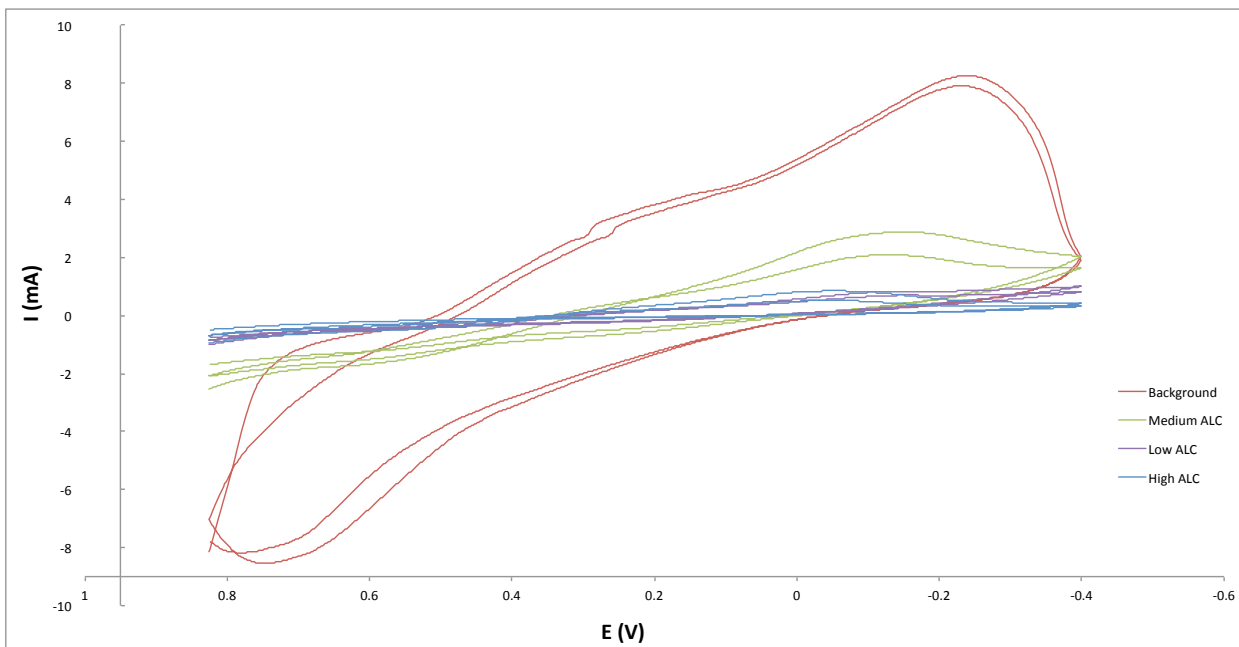


**Figure 3.1: Results showing decrease in Pani signal in pH 5.3 Phosphate Buffer (Medium in green is higher than low and high)**

This system gave way that there might be some slight unpredictability as to how ALC is interacting with the Pani. This unpredictability may be attributed to some sort of absorbance of ALC into the Pani matrix. As we will discuss later, the unpredictability may also be attributed to some sort of chemical reaction occurring. Figure 3.2 shows the same film grown and cycled from Figure 3.1, in first medium ( $1.853 \times 10^{-4}$  M), then low ( $4.634 \times 10^{-5}$  M), then high ( $7.414 \times 10^{-4}$  M) concentrations of ALC. This figure shows that the peak current around -0.2 V coming from the reduction of Pani, decreases further while being cycled in the lower concentration, and then decreases further during being cycled in a higher concentration of ALC. The decrease from medium to low is thought to come from when more ALC is added to the film. The Pani interacts further with the ALC to decrease the amount of current being produced from the redox of Pani.

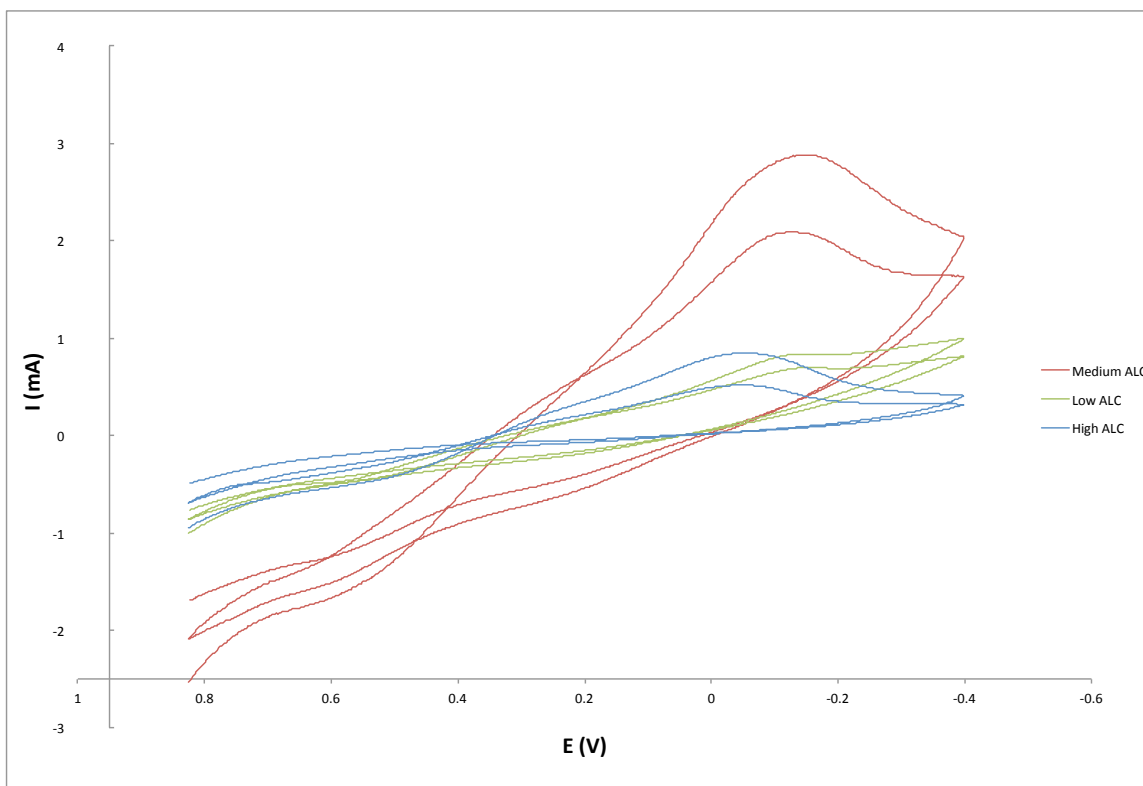


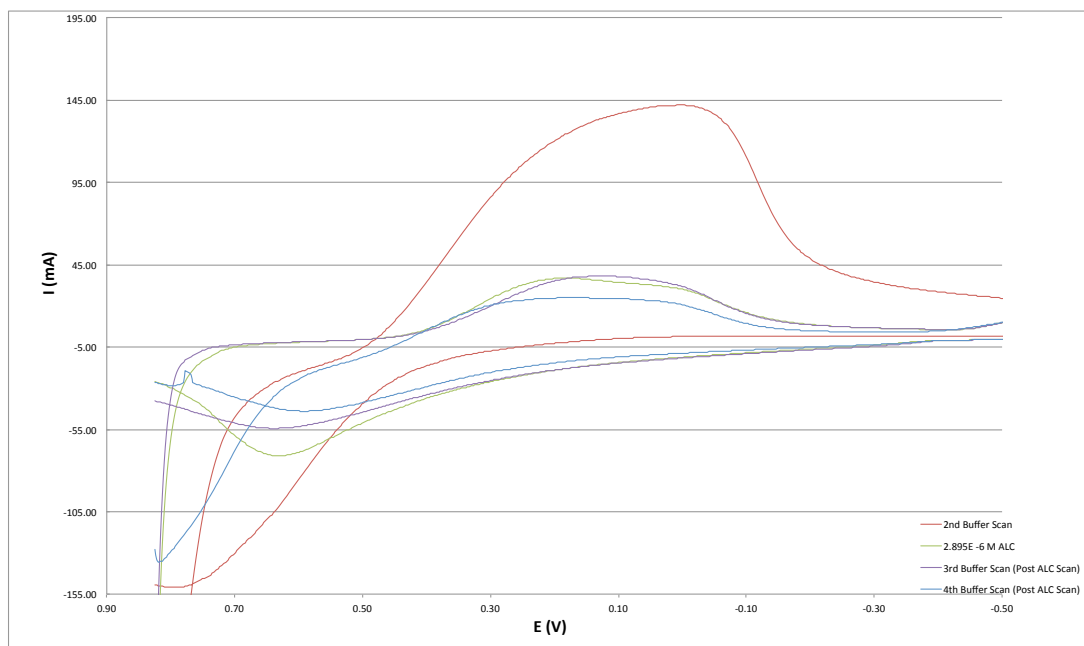
**Figure 3.2: Results of Pani cycled in low, medium, and high concentrations of ALC solution in pH 5.3 Phosphate buffer**

After the investigation of these happenings within the pH 5.3 phosphate buffer system it was thought that the pH may be too high in order to generate a Pani signal distinct enough to create a calibration curve able to sense exact concentrations of ALC in aqueous solution. Therefore, this led to the search to find a system with a slightly lower pH that would help Pani to conduct better at the surface of platinum, but also allow good reactivity with ALC. In choosing another experimental solution to work in at a lower pH my reasoning was that it needed to be a system showing a fair amount of conductivity, but presented a fair amount of safety in having no interaction with the Pani or with the ALC. Therefore, a universal buffer mixture with citric acid and sodium phosphate dibasic was

chosen as it consisted of a pH that was more conducive to reaching the goals just described.

## B.) Irreversible Reduction of Polyaniline

The universal buffer mixture at pH 4 provided a good electrochemical system in order to conduct experiments that showed the effects of ALC on the Pani electrode. In Figure 3.3, the overlaid results of a special experimental sequence involving multiple buffer scans described in the methods section are depicted. The first scan in buffer is not depicted because the first is the one that introduces the polymer to the system and does not give adequate information.



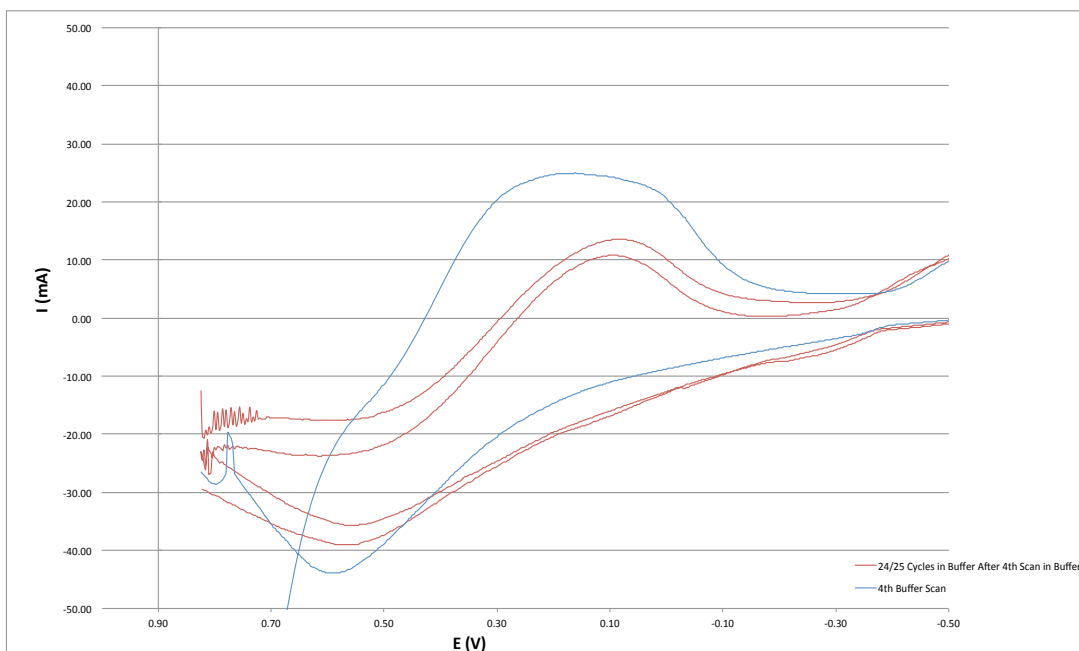
**Figure 3.3: Results of multiple buffer scans and ALC scan showing a decrease in Pani signal (1 mm Pt wire electrode used as working)**

Figure 3.3 shows the Pani signal from approximately +0.8 V to -0.2 V. The second buffer scan is depicted in red and the scan in pesticide solution in green. The

drop in signal current between the two scans is tremendous and due to the nature of Pani, it is unlikely this would happen between scans unless there was some sort of interaction happening. As well, after a scan in ALC solution the Pani electrode does not recover in current after being cycled multiple times in pH 4 buffer solution with no pesticide present, as can also be seen by the third buffer scan in purple and fourth in blue.

Following these scans, a longer scan was done for 25 cycles. This was done to see if the polymer would recover at all from the scan in pesticide, as in, would it “flush” the pesticide from the polymer matrix. If the polymer was able to “flush” the pesticide from its matrix, the pesticide is simply being absorbed. The result however was that ALC was not being absorbed and there was some other sort of interaction happening, which is seen in Figure 3.4.

In Figure 3.4 the blue line depicts the fourth scan in buffer and the two red lines show the twenty-fourth and twenty-fifth scans in buffer. The twenty-fourth is seen to be higher in current than the twenty-fifth, which shows qualitatively that the signal is indeed shrinking and that the reduction of Pani at the surface of platinum, in the presence of ALC is irreversible because Pani signals in an acidic media are known to increase if not for an interaction of some sort with another species.<sup>33</sup>



**Figure 3.4: Overlay showing no recovery of Pani after additional 25 cycles to fourth buffer scan  
(1 mm Pt wire electrode used as working)**

This concurs with the results of El-Shahawi et al and their work with ALC, showing that ALC itself presumably irreversibly reduces at the surface of HMDE.<sup>49</sup> If ALC itself irreversibly reduces electrochemically, than anything it interacts with chemically in a system will also irreversibly reduce because the ALC is the inhibiting factor on the electrochemical level. Due to the nature of Pani as a matrix, the location(s) of where ALC is interacting in that matrix cannot be known. For the purpose of this study it can be said that ALC is interacting at certain sites on the Pani matrix. We will further explore this interaction of Pani and ALC later on in this chapter.

### **C.) Analysis of Electrical Current Trends in Polyaniline Electrode**

Now that the basis of an interaction with Pani and ALC has been established, we can address the primary goals of this project, which was develop a way for ALC to be sensed electrochemically by the Pani. The way that this was done was through electrical current given off by Pani upon its interaction with ALC. Current was analyzed by looking at the peak reduction current of Pani located at  $\sim -0.2$  V within the experimental range. The reduction current was chosen because incremental decreases could be seen in the reduction peak of Pani at  $-0.2$  V; additionally the oxidation peak of Pani was often incomplete and sometimes non-existent in experiments.

In order to determine a trend in the electrical current produced by Pani I first collected a Pani baseline signal in pH 4 buffer and then moved to scanning the Pani electrode in a ALC solution of very low concentration ( $2.895 \times 10^{-6}$  M), then scanning the same electrode in a separate solution concentrated four times as much ( $1.158 \times 10^{-5}$  M), then scanning in another solution concentrated four times as large as the previous ( $4.634 \times 10^{-5}$  M). What this established was an experimental basis that allowed me to see what happened to the electrode with just a little amount at first to get an idea of the effect ALC had on Pani. Then increasing the concentration allowed me to see if the effect would continue. In my course of experiments I was able to generate a set of data that showed an overall decrease in electrical current put out by Pani cycled in the presence of ALC. Within correlation of my lab notebook and for the sake of brevity as they are discussed here, we will call these cycled films Pani A, B, and G. Films Pani C through F will be addressed later in this section.

Once this procedure was instituted, it was performed with the homemade platinum electrode as described before in the methods and growth was done up only to 100 mC. This electrode did not seem to provide enough of a platinum surface for the Pani to grow over and the film after a few scans fell off the electrode. This caused me to switch to platinum foil strip with a growing area of  $\sim 1 \text{ cm}^2$  per side of the foil. I grew this to 5 C and this provided a much larger and stable base for Pani to interact with the pesticide.

After instituting this procedure with the foil, results for Pani A were produced, as seen in Figure 3.5. Figure 3.5 shows only the third scan out of the three cycles. The results that are depicted in Figure 3.5 show that after the buffer scan, the peak current increased on the low ALC concentration scan ( $2.895 \times 10^{-6} \text{ M}$ ). This may be due to slight damage to the surface of the film during solution change between experiments. However, in general as more and more ALC is cycled with Pani A the peak current decreases and some interaction between ALC and Pani seems to be present.

The curve in Figure 3.6 shows the plot of peak current of Pani A versus concentration, which does show an overall decrease in peak current.

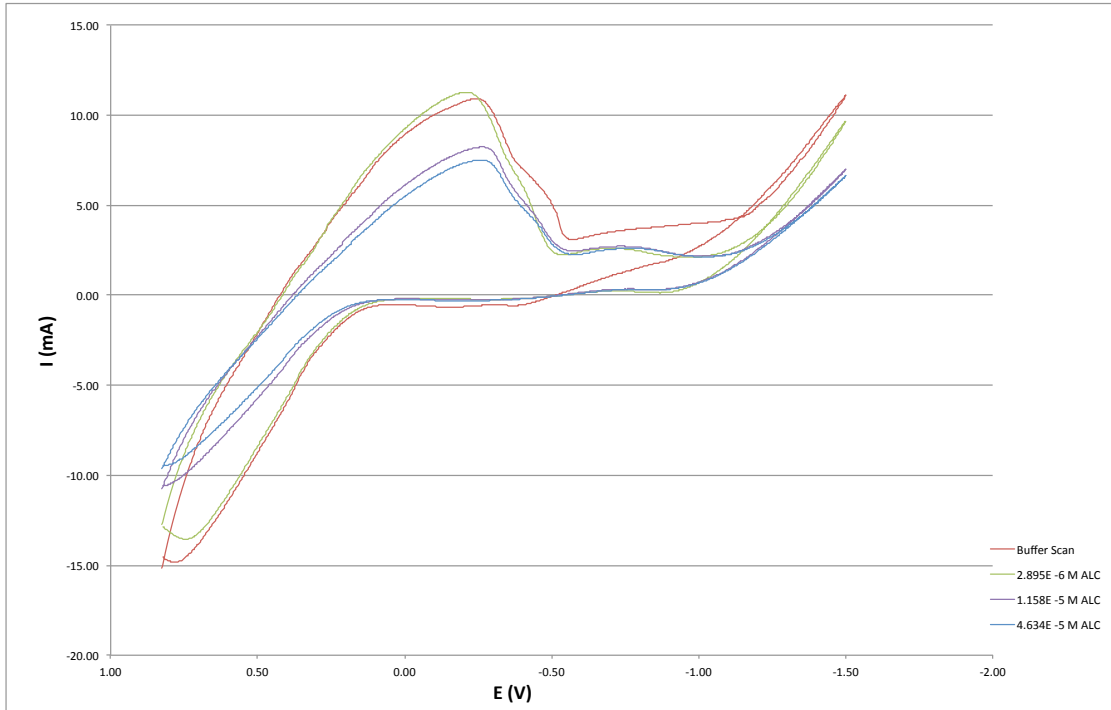


**Figure 3.5: Results from Pani A experimental sequence (Pt foil used as working)**

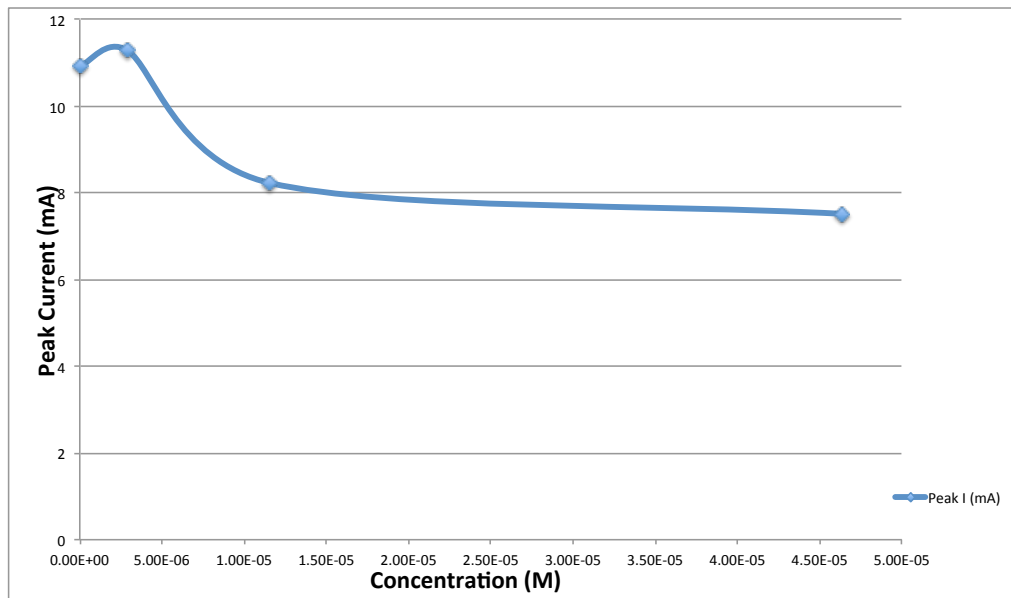


**Figure 3.6: Plot of peak current from Pani A sequence vs. concentration of ALC**

The next experiment immediately following was Pani B. Pani B showed no major signs of damage by flaking or by the appearance of the platinum surface



through the entirety of the experimental sequence. Figure 3.7 below depicts the overlaid results of the third cycle of each experiment performed with Pani B. The figure depicts a very nice incremental decrease in peak current with increasing concentration of ALC.

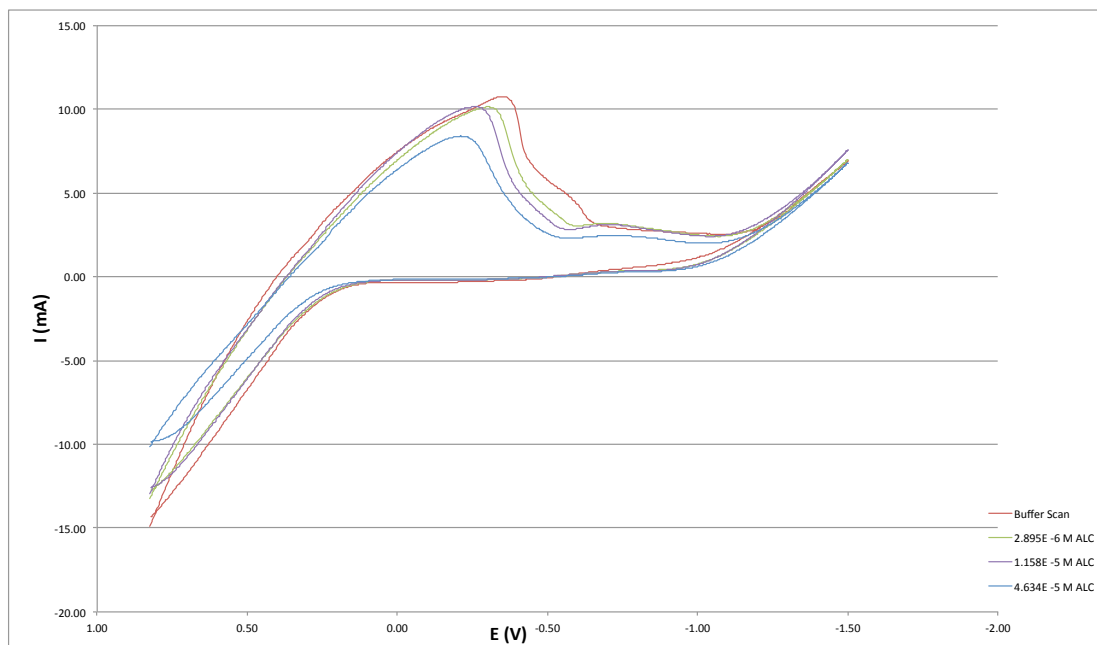


**Figure 3.7: Results from Pani B experimental sequence (Pt foil used as working)**

Figure 3.8 depicts the peak current from each Pani B experiment versus concentration of ALC. The figure shows that from this experimental decrease there is a nearly linear decrease in peak current with increasing concentration of pesticide. Reasons for the lack of total linearity may be due to systematic error by easy disturbance of the film during solution change between experiments

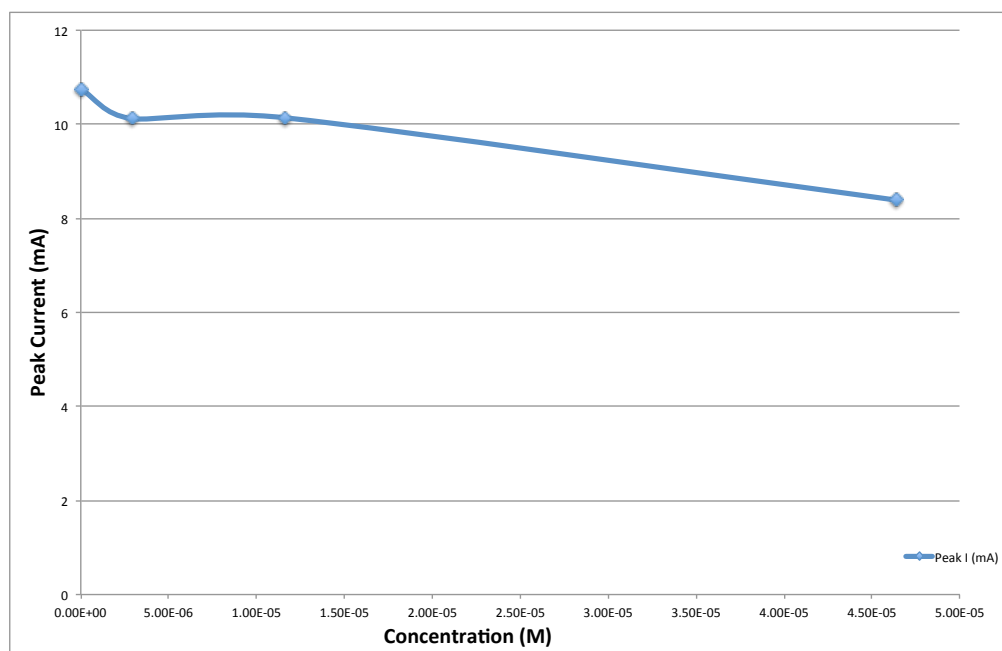


**Figure 3.8: Plot of peak current from Pani B sequence vs. concentration of ALC**

The third experiment in this analysis was Pani G. Pani G also showed an overall decrease in peak current with increasing ALC concentration. In Figure 3.9 the overlaid results of the third scan of each Pani G experiment are depicted. Pani G sustained little to no damage by flaking or exposure of platinum surface through the experimental sequence. The decrease between the buffer scan and the first ALC scan is very large and shows that there is an unpredictability to which sites on the polymer matrix are interacting with the ALC, as well as a to how many are interacting. The scans involving the medium ( $1.158 \times 10^{-5}$  M) and high ( $4.634 \times 10^{-5}$  M) concentrations of ALC show that the peak current signals are nearly the same. However, the Pani reduction peak signal for the scan involving the high concentrated solution is narrower where the reduction potential has shifted slightly more positive and the signal drops lower than the previous scan after the

reduction. These are all indications that further interaction is happening due to the presence of ALC.

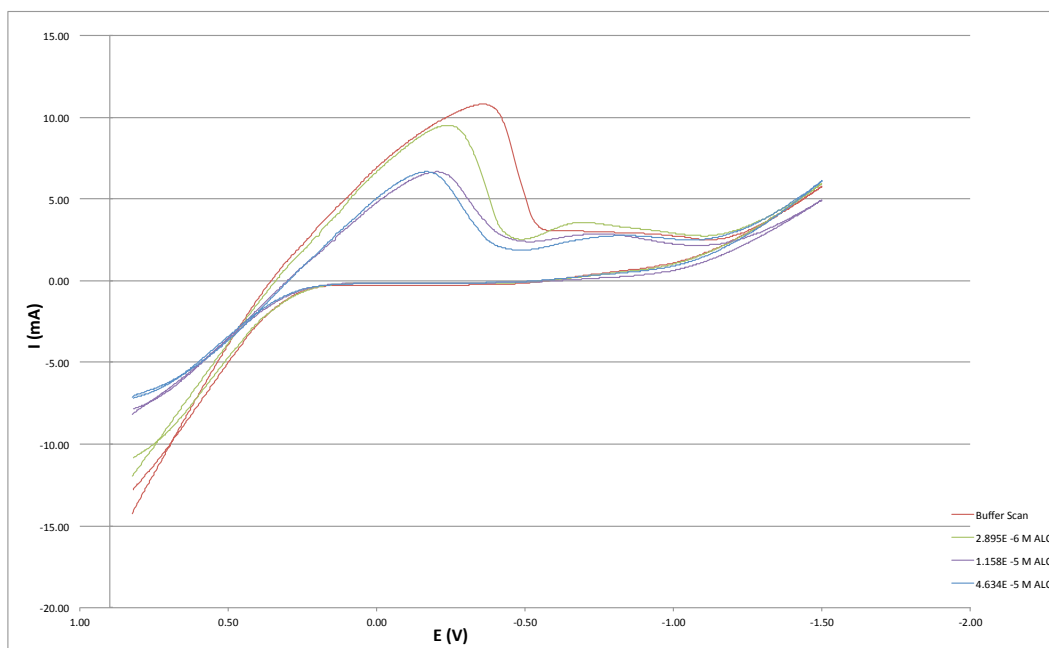


**Figure 3.9: Results from Pani G experimental sequence (Pt foil used as working)**

In Figure 3.10 the peak current of each experiment done with Pani G versus the concentration of ALC is depicted. It appears as though the curve increases with the last two experiments. However, these values are actually the same and the peak current stays at 6.66 mA between the medium and high concentrations. This could suggest that there is either some random error happening on the molecular level where the interaction between Pani and ALC is occurring or some kind reaction rate, kinetic effect. What may affect the kinetics is unknown. Overall the curve decreases with no fluctuation in current showing an increase.

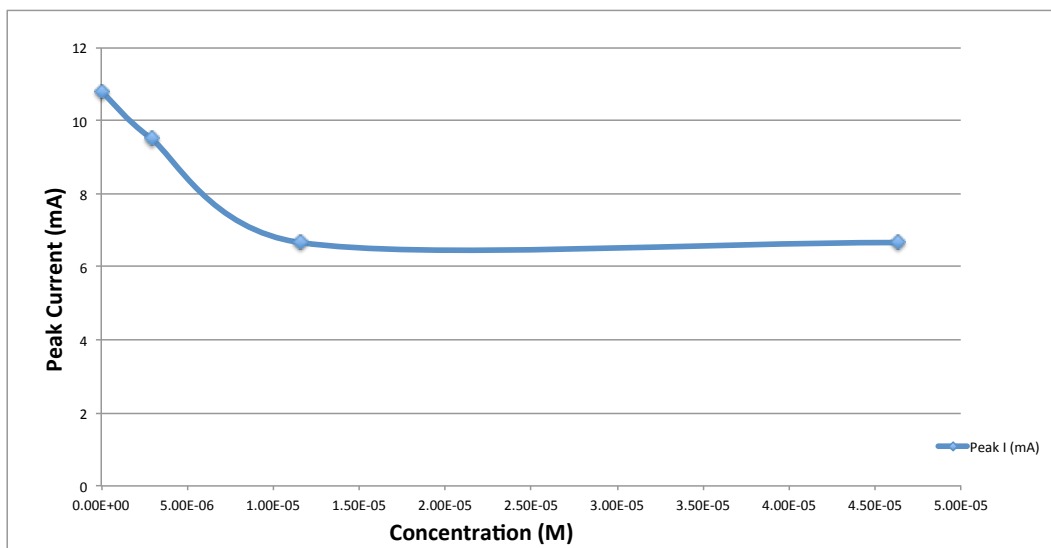


**Figure 3.10: Plot of peak current from Pani G sequence vs. concentration of ALC**

Because of the repeatability of these three experiments, the current trend for the sensitivity towards ALC in this interaction between Pani is a decrease. This current trend says that the resistance of the electrode is increasing (as stated before) and the conductivity is decreasing. Below in Figure 3.11, the average peak currents from experiments Pani A, B, and G are shown versus concentration of ALC with error bars. The error was calculated using the standard deviation of peak current at each concentration of ALC for the three films. Figure 3.11 is also a calibration curve for the detection of ALC by the Pani electrode. The largest error occurs at the medium concentration of ALC ( $1.158 \times 10^{-5}$  M) having a standard deviation of 1.743 mA. The smallest error is in the initial pH 4 buffer scan having a standard deviation of 0.0944 mA. The error occurring at this point in the sequence again may be due to film damage, random error, and the suggested kinetics inference.

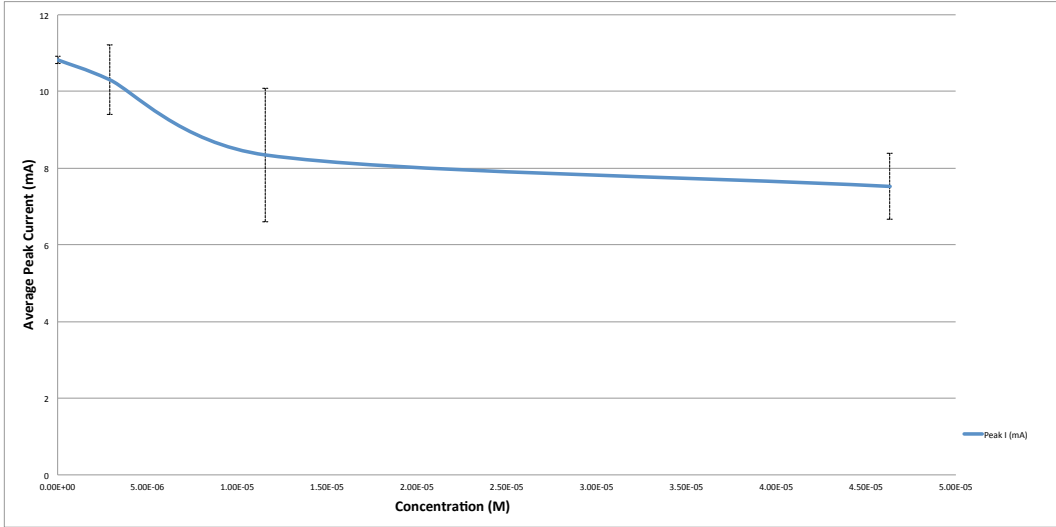


**Figure 3.11: Average of peak currents of Pani A, Pani B, and Pani G vs. concentration of ALC**

The film damage issue will now be addressed. In the case of Pani A and B, both had slight film damage based on visual inspection upon entrance to the first solution; both still showed a decrease in current with increased concentration of ALC. Films Pani C through F were complicated and showed visible damage; all showed slightly unpredictable current trends.

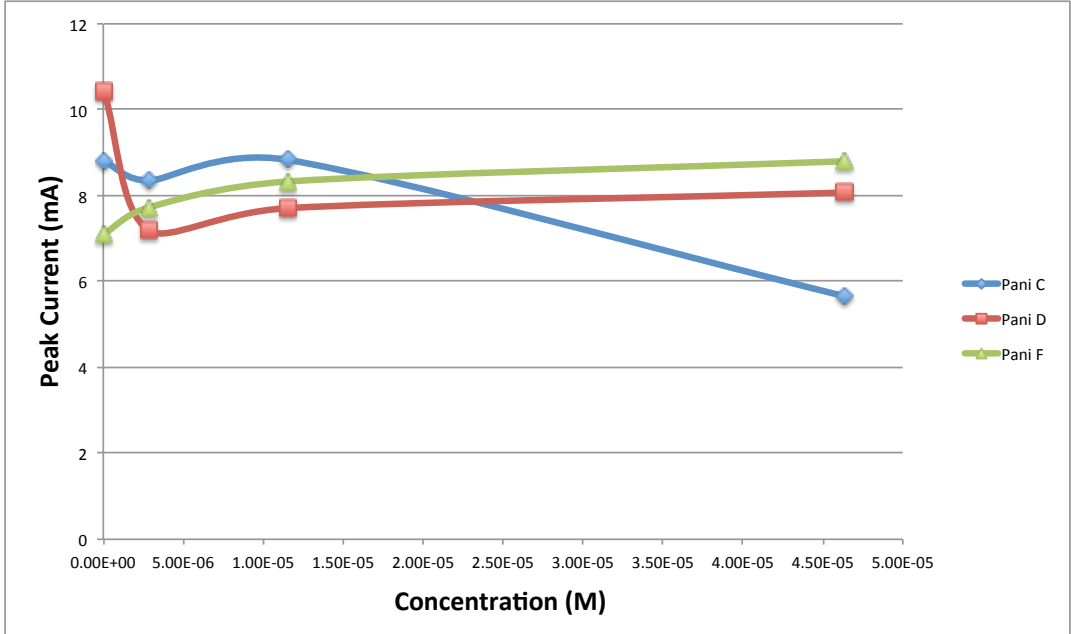


**Figure 3.12: Peak current vs. concentration of ALC for Pani C through Pani F**

Figure 3.12 shows the peak current vs. concentration of ALC for these films. Pani E is not included because such large film damage was sustained during the collection of the Pani baseline signal no further scans could be done. These current trends show an overall increase for Pani D and Pani F. However, Pani C shows to have an overall decrease, but does not fit the hypothesis of this study due to the very large amount of error in the curve. These pieces of data were excluded from the study in order to simplify the overall analysis. Due to the interest of time in this project, further studies need to be done to determine the reason for such irregular trends.

It seemed unlikely that, with the presence of an organic material with a fairly large structure, the current would increase upon addition because of the lack of conjugated bonds in ALC. After the experimental sequence with Pani G, I purposely scratched the film with a pipette enough to show the surface of platinum and performed a scan with the  $7.414 \times 10^{-4}$  M ALC stock solution to see if the current would continue to decrease, as it should with increasing concentration of ALC.

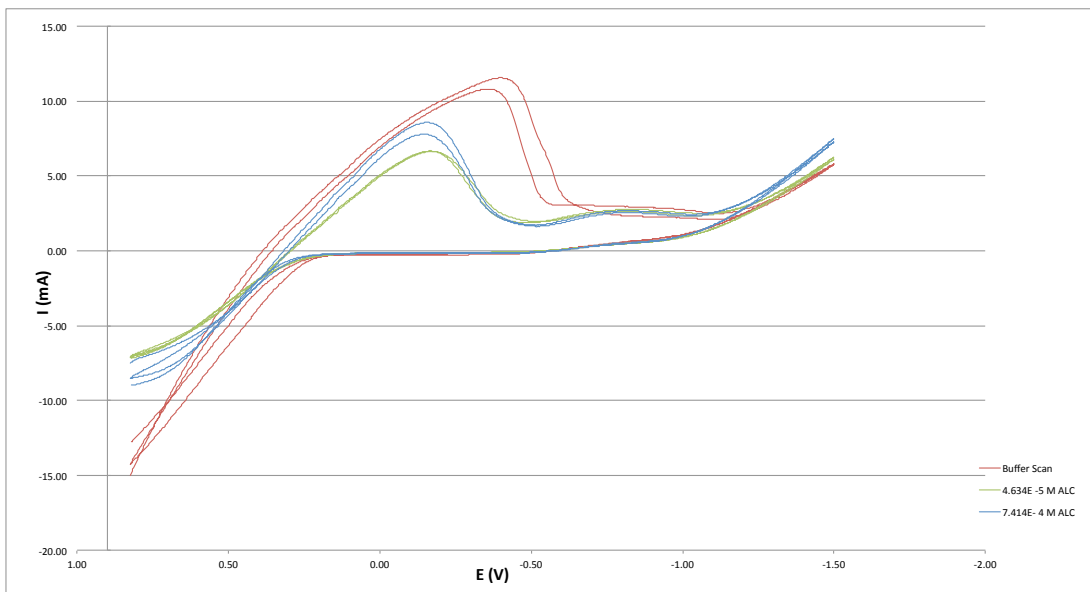


**Figure 3.13: Results of film damage test**

Figure 3.13 above depicts the initial buffer scans (second and third), the preceding pesticide scan (only third) in  $4.634 \times 10^{-5}$  M, as well as the second and third cycles in the stock solution. The cycle higher in current during the stock solution scan is indeed the third scan, which showed that with film damage the current increases. This is most likely due to the exposure of platinum, which would increase the current of the system in its entirety due to increased electrolytic activity with the platinum. Figure 3.14 shows a picture representing the difference between a damaged and undamaged Pani film.



**Figure 3.14: Image showing a damaged and non-damaged PANI films**

It should be noted that in the experiments, whose figures are shown in this section, there is a shift in the PANI reduction potential. As the current decreases with increasing concentration of ALC, the potential becomes slightly more positive. This may be due to a variance in oxidation state of PANI during experimentation while electrochemically cycling. Further reasoning for the shift in PANI redox potential is covered briefly in Chapter 1, section C-2. It should also be noted that electrochemical cycling of PANI might affect the layering network of the polymer when it grows layers parallel to the substrate. The change in the layering at the surface of PANI may indeed have some effect on the conductivity of the system, however, whether this is a factor or not in this study is unknown.



#### **D.) SEM and FTIR Experiments**

After investigating the sensitivity of the Pani electrode, further experiments were done with SEM and FTIR in order to understand the inferred interaction occurring between Pani and ALC.

We will first look at the SEM images taken on two samples of Pani, prepared as described in the methods section. Figures 3.15 and 3.16 show control Pani in pH 4 buffer and Pani cycled in ALC under an SEM at 100 nm resolutions. The images both show individual Pani fibers interwoven together in a random matrix. The difference that infers the interaction occurring is seen by the ridges that appear on the individual Pani fibers. They seem to be evenly occurring across each fiber, but each fiber is not entirely covered in ridges, which would agree with the notion that the interaction is random and thus there would be some random error as well.

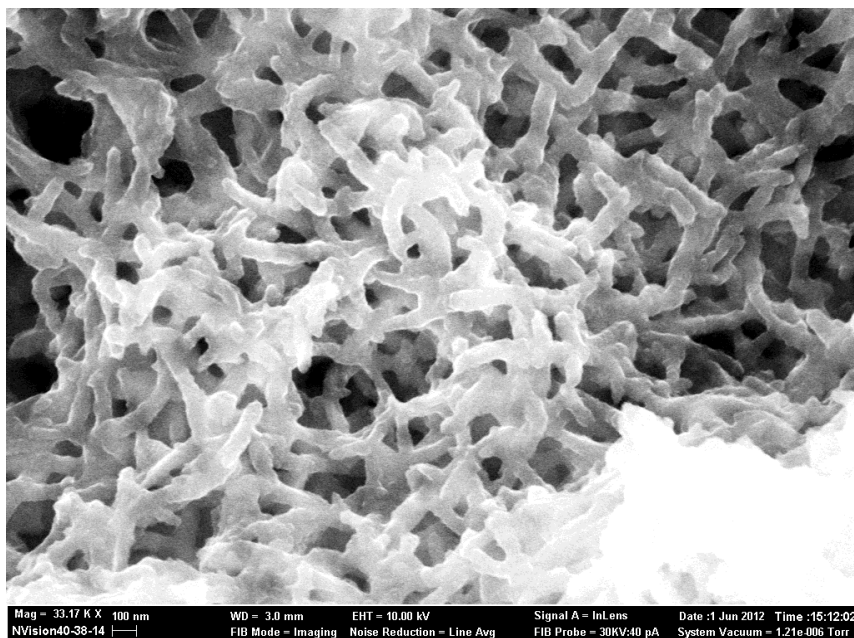


**Figure 3.15: SEM image of Pani at 100 nm resolution**

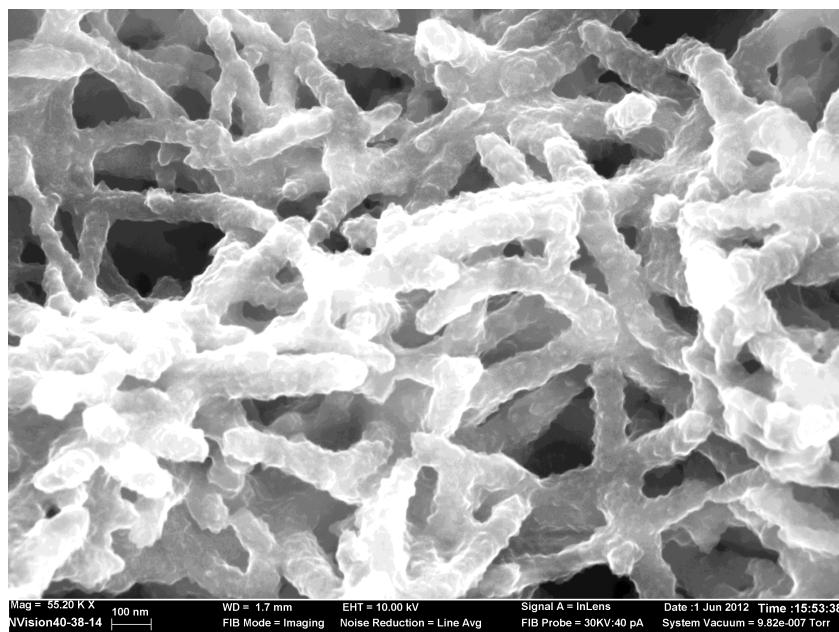


**Figure 3.16: SEM image of Pani cycled with ALC at 100 nm resolution**

The next two images are Figures 3.17 and 3.18, which show the control Pani and Pani cycled with ALC at 1  $\mu\text{m}$  resolution. These two images depict a “zoomed out” image showing a bigger picture to how ALC is affecting the Pani. There are some visible morphological differences between Pani cycled with ALC and the control Pani, where the image of the Pani control seems to be more “full”; as in there are less holes in the matrix overall. Whereas in the image of Pani cycled with ALC there are more pockets and holes between intertwined fibers. The fibers within the Pani control sample seem more “tangled”, whereas in the Pani cycled with ALC fibers seem less “tangled” and more uniform.

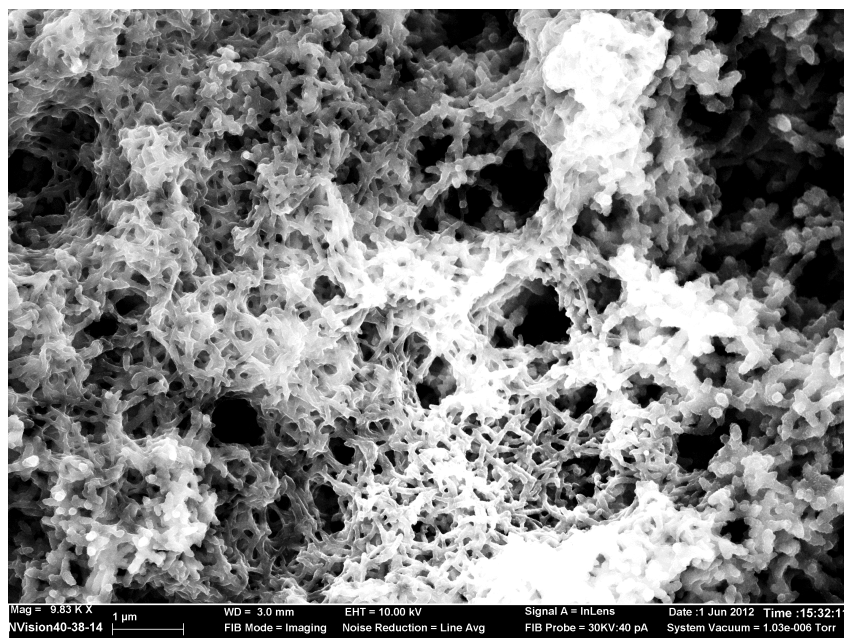


**Figure 3.17: SEM image of Pani at 1  $\mu\text{m}$  resolution**

The differences as described above in these SEM images give more clarity to the notion that there was some interaction occurring, which led me to think that with another instrumentation method I could start to even describe the interaction with a reaction mechanism. However, due to the nature of Pani and the way it grows over a substrate in intertwined parallel layers, these morphological changes as described may be due to a change in the layering of Pani by simply cycling in buffer solution. A way to discover if these morphological changes are chemical between Pani and ALC are to perform control experiments. An example of this control experiment would be done by cycling Pani, in the same way as was done in ALC solution, in only buffered solution. After performing SEM, no difference between the controls and the sample cycled in ALC would attribute the differences to be due to a change in layering of Pani, where the opposite would

suggest chemical interactions. However, in order to confirm a chemical interaction these changes need to be seen on the molecular level, which can be done by FTIR.

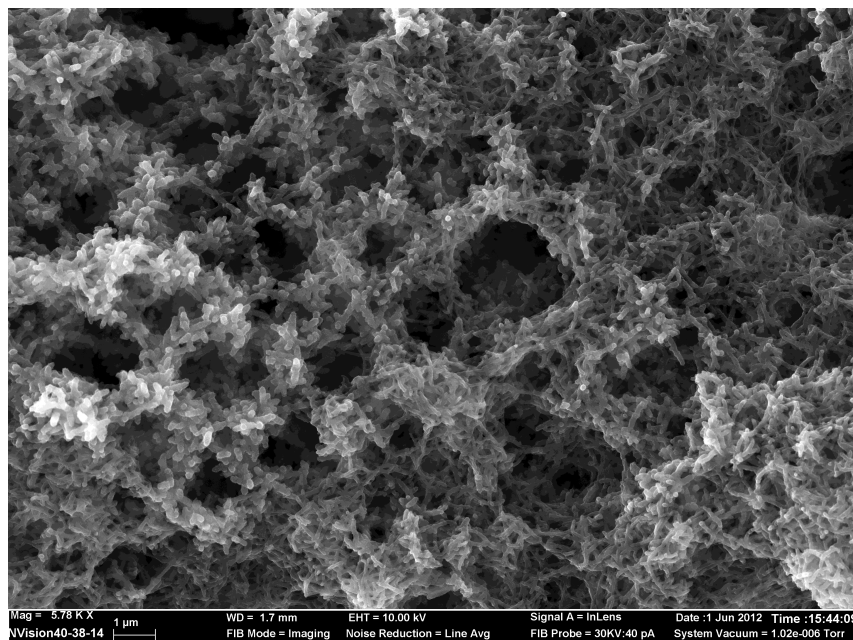


**Figure 3.18: SEM image of Pani cycled with ALC at 1  $\mu\text{m}$  resolution**

In addition to the SEM images, FTIR spectra provided information that also showed substantial differences between before and after Pani interactions with ALC. DRIFT spectroscopy was used to obtain enough sensitivity to samples in order to make absorption band assignments and without severely altering the physical state of the solid sample. All figures below show a  $\text{CO}_2$  peak between  $2300$  and  $2400\text{ cm}^{-1}$  due to atmospheric interactions. All assignments were made using a table of characteristic IR absorption frequencies.<sup>50</sup>

Figure 3.19 provides DRIFT spectra of just Pani. The peak assignments that are inferred from analysis are an N-H bend that can be seen at  $\sim 1600\text{ cm}^{-1}$ , which is absolutely essential to the backbone of the Pani chain. There is a possible C-N

vibration around  $\sim 1000\text{ cm}^{-1}$ , which would correlate to the aromatic ring connection to the nitrogen forming the essential makeup of the Pani monomer, aniline. However, between  $1500$  and  $1000\text{ cm}^{-1}$  the region is unlike the regions in Figures 3.19 through 3.21 which causes me to think that this is a fingerprint region for Pani and is characteristic of its bonding structure. Due to time constraints on this project this was not investigated and is something for future work.

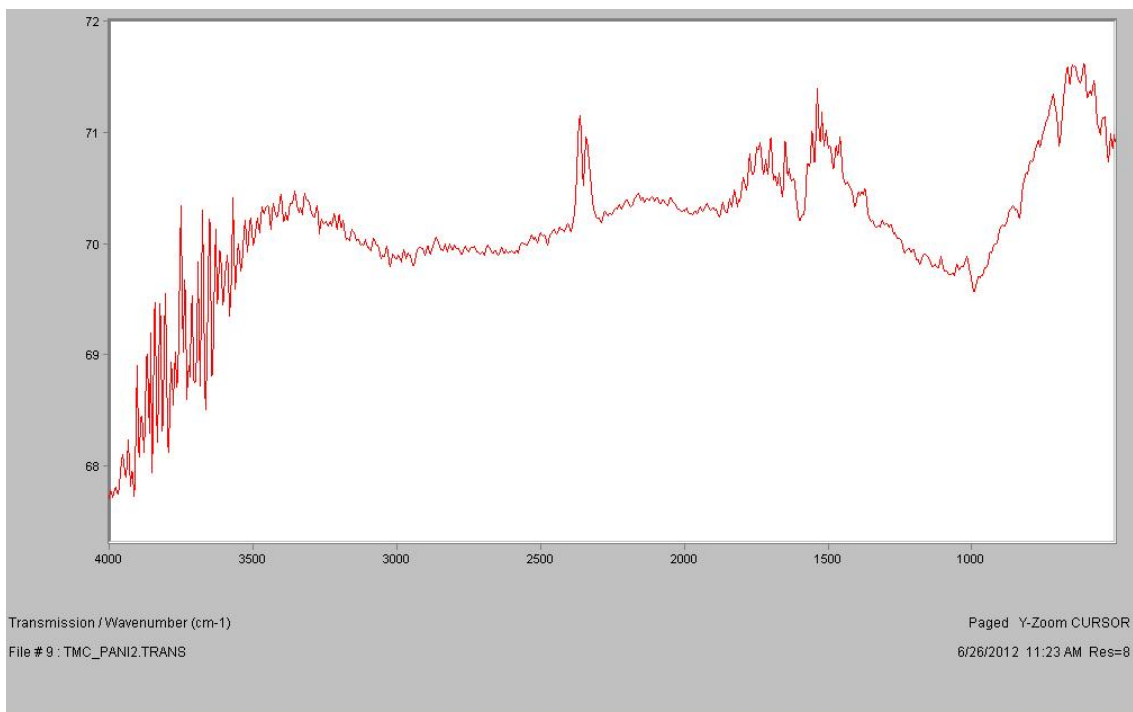


**Figure 3.19: DRIFT IR spectra of Pani sample prepared 06/13/12**

Figure 3.20 shows an FTIR spectrum of ALC published by NIST. This spectrum is present in order to reference known IR absorption bands of ALC. The following three figures (3.21 – 3.23) are figures that show DRIFT spectra of Pani that were prepared on three different dates. This was done in order to show that the spectra were consistent, as well that the interaction was repeatable.

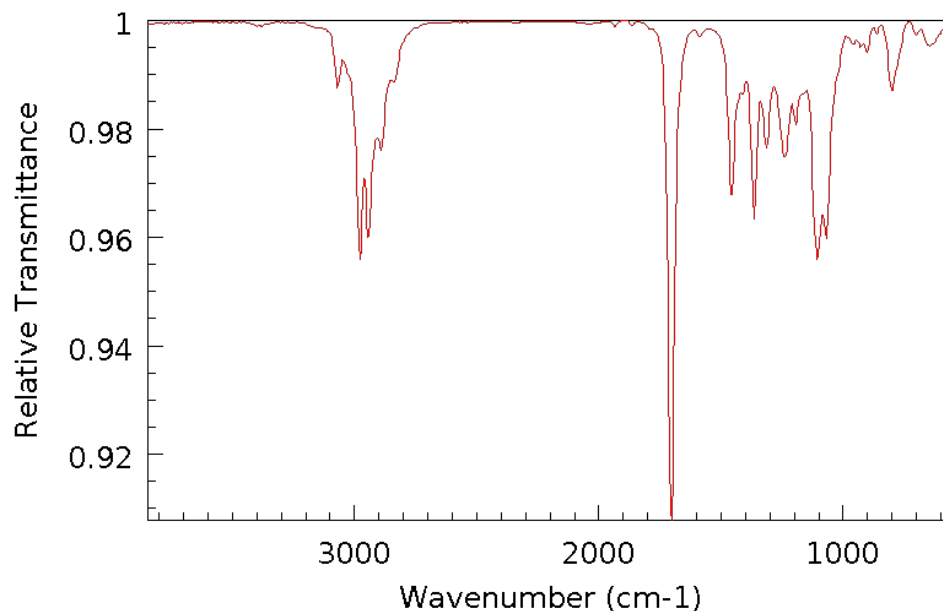


**Figure 3.20: FTIR spectra of alachlor.<sup>51</sup>**

Figure 3.20 shows the signature FTIR absorption bands of ALC, which are as follows: the N-H stretch around  $3000\text{ cm}^{-1}$  for the amide bond in the chemical structure, the C=O stretch at  $\sim 1700\text{ cm}^{-1}$  correlating to the amide carbonyl, there are a few C=C aromatic stretches at  $\sim 1500\text{ cm}^{-1}$  and  $\sim 1400\text{ cm}^{-1}$ , the band with two peaks between  $1100$  and  $1000\text{ cm}^{-1}$  correlate C-O stretching which represent the ether group (R-O-R'), a few small peaks between  $1200$  and  $1300\text{ cm}^{-1}$  may correlate to C-N vibrations, as well there is a small sharp peak between  $700$  and  $800\text{ cm}^{-1}$  which correlate to the tri-substituted aromatic bending.

The absorption bands for the following spectra are nearly the same as the Pani spectra with some minor differences, some to which include the assignments made to the ALC spectra in Figure 3.20. First I will note the Pani bands that can still be seen on these spectra. The band at  $\sim 1600\text{ cm}^{-1}$ , correlating to the N-H in Pani, remains. Figure 3.20 shows the peak that was seen at  $\sim 1000\text{ cm}^{-1}$  indicating a

possible C-N vibration. The vast majority of the noise that was seen between 1500 and 1000  $\text{cm}^{-1}$  disappears in all of the spectra and is replaced by a few different peaks. The first of these peaks is somewhere in between 1400 and 1300  $\text{cm}^{-1}$  showing a possible C-H bend which would correlate to ethyl or methyl groups present in the new structure, which, if ALC was chemically reacting with Pani, there would now be ethyl groups related to the ALC structure. Between 1200 and 1100  $\text{cm}^{-1}$  there are two, sometimes three peaks, which possibly indicate a C-O stretch also coming from the ALC structure correlating to an ether group. There is a slight shift from the bands seen in Figure 3.20, where this shift may be due to the chemical interaction between ALC and Pani. There are also a few small peaks at  $\sim 800 \text{ cm}^{-1}$  and  $\sim 750 \text{ cm}^{-1}$  which would correlate to aromatic peaks being tri substituted and di substituted, respectively. These also correlate to the ALC structure where the aromatic ring in the pesticide is tri substituted with two ethyl groups and a nitrogen atom.

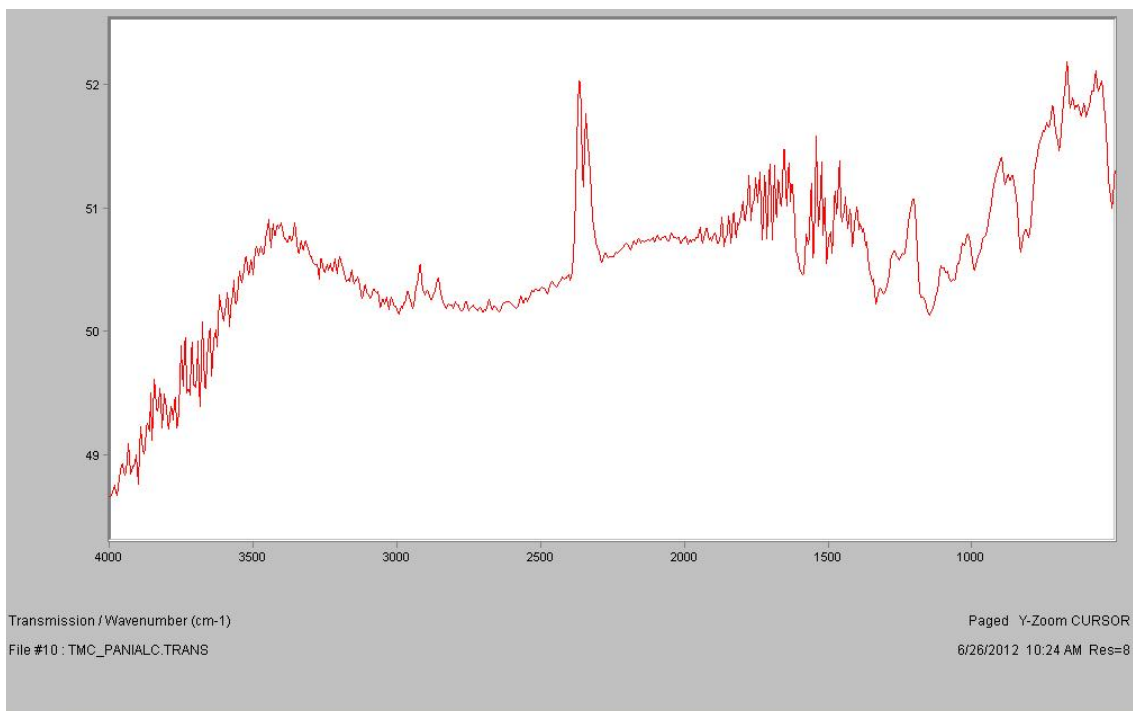


**Figure 3.21: DRIFT IR spectra of Pani cyclized with ALC prepared 06/08/12**

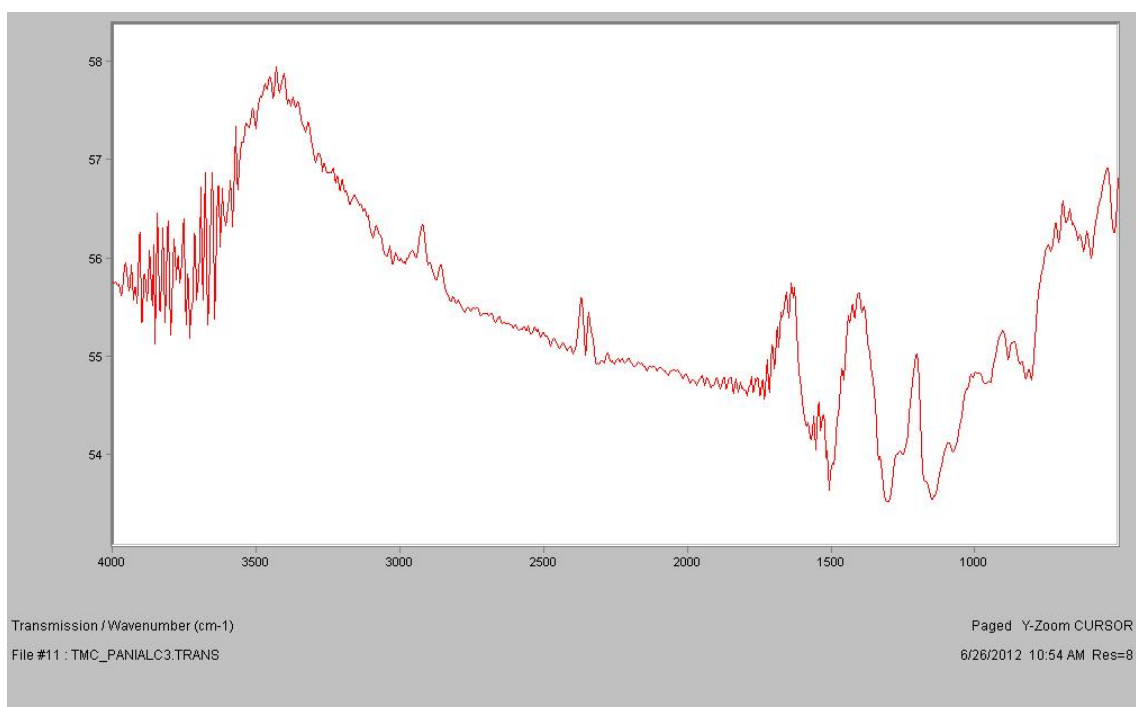


**Figure 3.22: DRIFT IR spectra of Pani cyclized with ALC prepared 06/13/12**



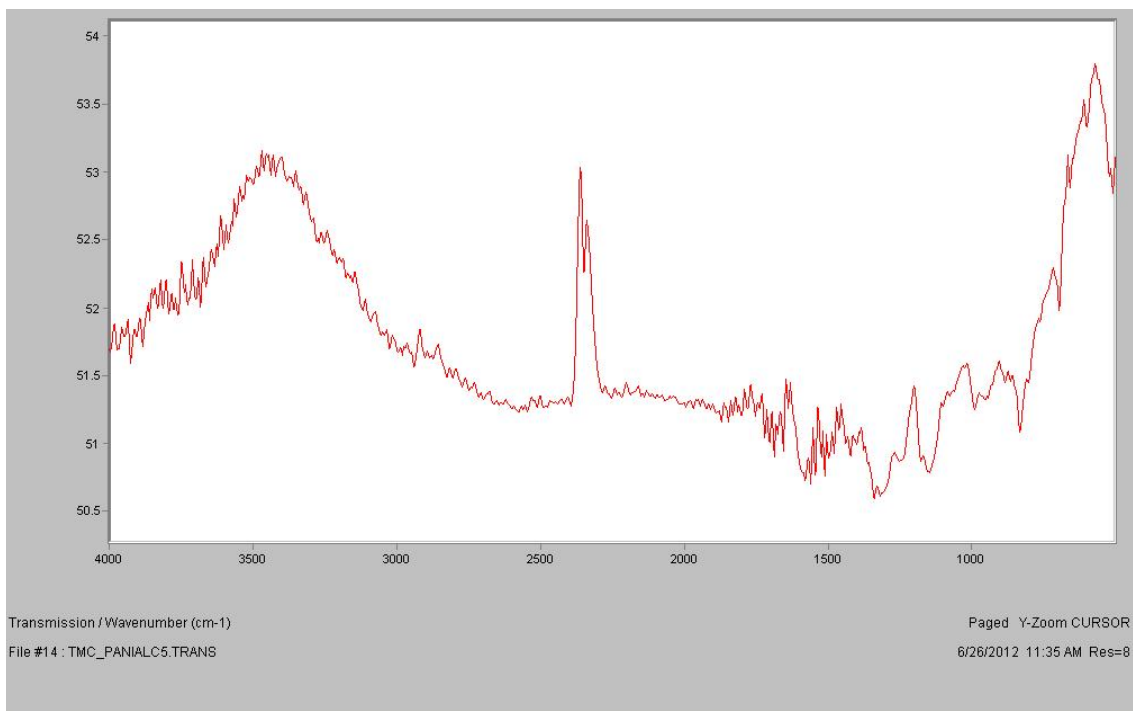


**Figure 3.23: DRIFT IR spectra of Pani cycled with ALC prepared 06/15/12**

There are however a few missing elements to the spectra, which may be due to sample preparation, some systematic error in drying, and sample extraction by scraping of the film. The missing elements are an O-H stretch around  $\sim 3000\text{ cm}^{-1}$ , which would correlate to the mechanism proposed in the next section, inferring the possibility that ALC has already been reduced electrochemically and then reacted with Pani. If this is not the case then a distinct C=O at  $\sim 1700\text{ cm}^{-1}$ , as seen in Figure 3.20, would appear, which would correlate to an unreduced ALC chemically reacted with Pani. However both of these elements are missing and are for investigation in future work.

### E.) Reaction of Amines with Chloroacetyl Chloride

Figure 3.24 depicts the organic synthesis of a compound known as lidocaine.<sup>52</sup> The amine portion of 2,6-dimethyl aniline reacts with the chloroacetyl functional group to produce an amide bond. Inspection of ALC shows a similar chloroacetyl substructure involving  $-C(O)CH_2Cl$ , which may be able to react with amines. The following section outlines how this may occur.

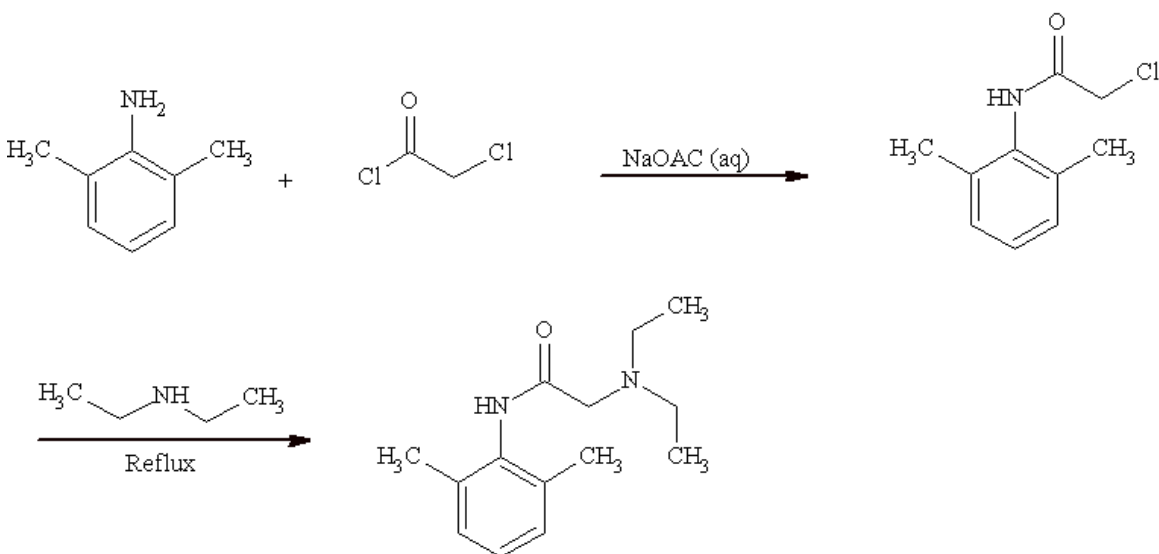


**Figure 3.24: Synthesis of Lidocaine**

### F.) Interaction of Polyaniline with Alachlor

The observed reactivity of 2,6-dimethyl aniline with chloroacetyl chloride, suggests that Pani may react with ALC as shown in Figure 3.25. This mechanism shows that the chloroacetyl functional group on the ALC, similar to the substructure outlined in section E, reacts with an amine in the Pani chain. This reaction is based off of an  $S_N2$  model organic reaction involving amines and alkyl halide functional groups.<sup>53</sup>

The 2<sup>o</sup> amine in the Pani chain, the emeraldine form is shown due to the acidity and abundance of lone pairs on the amines, is the attacking group or nucleophile. This is favored as the attacking group due to the nature of the functional group having higher reactivity as a Lewis base, defined with a lone pair of electrons. The leaving group on the ALC is a chloride making it a 1<sup>o</sup> alkyl halide, which would have decent reactivity with an amine.

The 2<sup>o</sup> nature of an S<sub>N</sub>2 reaction decreases the argument for this type of reaction because the solvent is protic, or water based, and most 2<sup>o</sup> S<sub>N</sub>2 reactions occur in aprotic solvent systems. Another factor against this mechanism is the sterics of the system. Pani is a highly aromatic system with many branches and fibers; as well ALC is an aromatic compound with many substituted groups, which sets it up for a possible intra-molecular reaction.

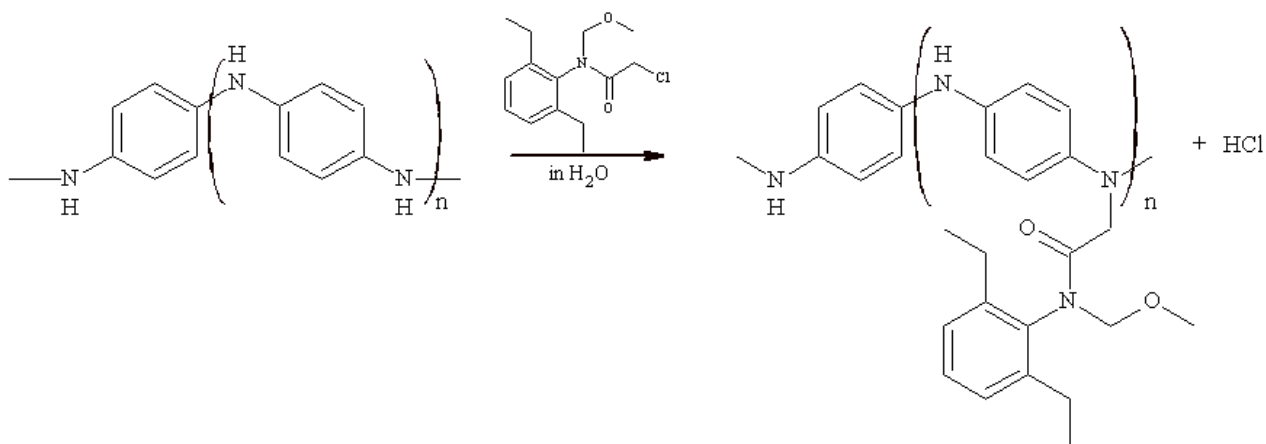


**Figure 3.25: Proposed reaction mechanism of Pani with ALC**

Figure 3.25 shows a chemical reaction that precedes an electrochemical reduction of ALC at -1.3 V. However, the electrochemical reduction of ALC is also possible, as outlined by El-Shahawi et al., depicted in Figure 3.26.

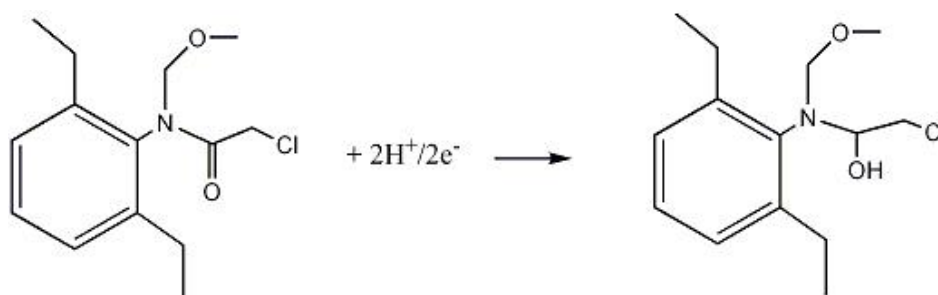


**Figure 3.26: Proposed reaction mechanism of the reduction of ALC by El-Shahawi et al.<sup>49</sup>**

The mechanism depicted in Figure 3.26, can be applied to the Pani ALC complex, resulting in a reduced carbonyl bond to form a hydroxide functional group. This is represented in the form of a chemical structure in Figure 3.27. Due to time constraints in this project the determination of whether this is in fact occurring, is a topic for future work. In the future, to determine whether the mechanism is indeed chemical as expressed by Figure 3.25, experiments could be done by simply collecting a Pani electrode baseline signal, taking the electrode out to sit in solution with ALC for some period of time followed by cycling in the redox range of Pani only, absent of ALC. A decrease in current would show the reaction to be chemical.

The nature of Pani as a matrix of intertwining fibers still leaves a chance of the proposed mechanism in Figure 3.25 to occur at certain active sites in the polymer. Figure 3.27 is a diagram showing the probability of an active Pani chain reacting with an ALC molecule.

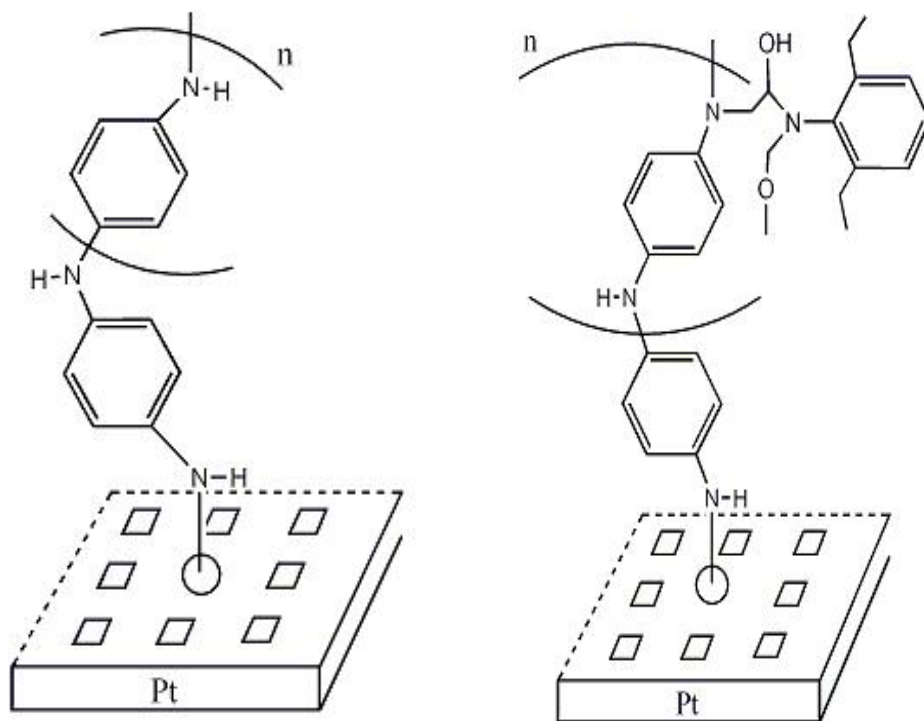


**Figure 3.27: Diagram showing attachment active Pani chain to platinum and reaction of that chain with ALC**

The platinum substrate is depicted with a grid of small squares that represent the attachment of Pani chains that are inactive sites for reaction with ALC; whereas the circle in the center depicts an active Pani chain undergoing reaction with ALC by the described mechanism in Figure 3.25. The grid does not in anyway depict an analytical study. This is merely a way of representing the qualitative idea of the proposed reaction. Understanding what sites are active and inactive is a completely random process and at this point it is impossible to tell which ones are active and inactive, as well as how many of each. This is also a topic for future work.

## **CHAPTER 4: CONCLUSIONS AND FUTURE WORK**

### **Conclusions:**

A correlation was made between electrical current transmitted by the Pani electrode during electrochemical experiments with concentrations of ALC. This led me to see that there was a possible irreversible reaction occurring with Pani because of the decrease in electrical signal produced by the Pani electrode.

Moving forward, it was assumed there was an interaction proceeding between Pani and ALC. Experiments conducted produced correlation between the magnitude of electrical current produced by the Pani electrode and concentration of ALC in an analytical study; thus giving the simple workings of an electrochemical sensor by a decrease in electrical current with increasing concentration of ALC.

By investigation with SEM and DRIFT IR spectroscopy it was found that there were indeed changes occurring in the system when Pani was cycled in the presence of ALC. This led to the actual proposal of a reaction occurring. Whether this is electrochemical or chemical is yet to be confirmed. The experiments in this study infer that the mechanism of reaction is a chemical reaction between Pani and the electrochemically reduced ALC. However, this does not rule out the possibility of an electrochemical reaction between Pani and ALC.

A selective Pani chain diagram is also proposed in order to illustrate how the ALC may be attaching to the chain at specific, active Pani sites. However, it is not known which sites and how many are being affected and reacted with pesticide.

In conclusion, this project by proof of concept met the goals and descriptions from the first chapter of this thesis. Thus the thesis statement has been fulfilled in this work.

### **Future Work:**

If this work is to be continued, there are many different systematic errors to which could be improved upon and many random errors that could be investigated with more time and resources available.

I mentioned an absorption factor between the polymer and the pesticide earlier in my discussions where the polymer could actually also be holding the ALC in pockets along the chain due to charge interactions. This absorption factor is one that can be investigated in the future by post reaction treatments with various types of solvents and further spectroscopic studies.

An analytical study can be done in the future to determine an actual detection limit of this sensor and reduce the error in the linearity of the calibration curve.

An optimization of coulombic growth of Pani with pesticide detection can be done to assure the appropriate amount of Pani needed for best sensitivity to ALC. As well, the optimization of the pH of the system for best conductivity of Pani with reactivity of ALC can also be investigated further in order to assure optimal sensitivity.

All experiments were done at room temperature however not all aqueous water sources sit at room temperature and so a thermodynamic study with system

temperatures could be conducted to observe trends between temperature and sensitivity in the system with Pani and ALC.

Investigation of morphological changes in Pani by performing control experiments and then comparing through SEM is also a topic for future work

Further spectroscopic techniques such as UV-VIS along with IR could be investigated for continued development to the proposed reaction mechanism between Pani and ALC. As well, further experimentation is needed to confirm the identity of the reaction between ALC and Pani as chemical or electrochemical.

A decrease in the amount of film damage during experimentation can be investigated to avoid experiments like that of Pani C through Pani F, which caused them to be unusable for analytical studies. This investigation will also be useful in decreasing the large error in peak current of Pani vs. concentration of ALC in order to optimize the sensitivity of the sensor.

A few more general ideas for future work would be investigate cheaper and more efficient electrode substrates to grow polyaniline over that would be disposable such as aluminum or nickel. Also, expanding out from alachlor to see what other classes of pesticides are able to interact with polyaniline would grow the versatility of this type of electro-analytical sensor.



## **CLOSING REMARKS**

This thesis was a learning experience to which I benefited most by the process of having to develop my own research project and seeing it through to fruition. It was extremely difficult to even come up with a topic, but once the process was moving, my procedures were defined, and I was generating data it became exciting. I truly feel that even though there were many errors, and still many unknowns in this project, it was a great success.

## REFERENCES

1. Conner, T. M., Pesticide Field Detection Methods. University of Maine. : 2011.
2. Alachlor Special Review Position Document 1. Agency, U. S. E. P.; Substances, O. o. P. a. T., Eds. U.S. Government Printing Office: Washington D.C., 1984.
3. *Alachlor in Drinking-water; Background document for development of WHO Guidelines for Drinking-water Quality*; World Health Organization: Geneva, 2003.
4. Agency, U. S. E. P., National Primary Drinking Water Regulations.
5. Tankiewicz, M.; Fenik, J.; Biziuk, M., Solventless and solvent-minimized sample preparation techniques for determining currently used pesticides in water samples: A review. *Talanta* **2011**, *86*, 8-22.
6. Hauser, B.; Popp, P.; Kleine-Benne, E., Membrane-assisted solvent extraction of triazines and other semi-volatile contaminants directly coupled to large-volume injection-gas chromatography-mass spectrometric detection. *Journal of Chromatography A* **2002**, *963* (1-2), 27-36.
7. Zapf, A.; Heyer, R.; Stan, H. J., RAPID MICRO LIQUID-LIQUID-EXTRACTION METHOD FOR TRACE ANALYSIS OF ORGANIC CONTAMINANTS IN DRINKING-WATER. *Journal of Chromatography A* **1995**, *694* (2), 453-461.
8. Ballesteros, E.; Parrado, M. J., Continuous solid-phase extraction and gas chromatographic determination of organophosphorus pesticides in natural an drinking waters. *Journal of Chromatography A* **2004**, *1029* (1-2), 267-273.
9. Liu, W. M.; Hu, Y. A.; Zhao, J. H.; Xu, Y. A.; Guan, Y. F., Physically incorporated extraction phase of solid-phase microextraction by sol-gel technology. *Journal of Chromatography A* **2006**, *1102* (1-2), 37-43.
10. Hu, Y.; Wang, Y.; Hu, Y.; Li, G., Liquid-liquid-solid microextraction based on membrane-protected molecularly imprinted polymer fiber for trace analysis of triazines in complex aqueous samples. *Journal of Chromatography A* **2009**, *1216* (47), 8304-8311.
11. Zhou, Q. X.; Xiao, J. P.; Wang, W. D.; Liu, G. G.; Shi, Q. Z.; Wang, J. H., Determination of atrazine and simazine in environmental water samples using multiwalled carbon nanotubes as the adsorbents for preconcentration prior to high performance liquid chromatography with diode array detector. *Talanta* **2006**, *68* (4), 1309-1315.

12. Hulanicki, A.; Glab, S.; Ingman, F., CHEMICAL SENSORS: DEFINITIONS AND CLASSIFICATION. *Pure and Applied Chemistry* **1991**, *63* (9), 1247-1250.
13. Bard, A. J.; Faulkner, L. R., *ELECTROCHEMICAL METHODS: Fundamentals and Applications*. 2nd ed.; John Wiley & Sons, Inc.: New York, 2001.
14. Letheby, H., On the production of a blue substance by the electrolysis of sulphate of Aniline. *Journal of the Chemical Society* **1862**, *15*, 161.
15. Mizoquchi, T.; Adams, R. N., ANODIC OXIDATION STUDIES OF N,N-DIMETHYLANILINE .1. VOLTAMMETRIC AND SPECTROSCOPIC INVESTIGATIONS AT PLATINUM ELECTRODES. *Journal of the American Chemical Society* **1962**, *84* (11), 2058-&.
16. Huang, W. S.; Humphrey, B. D.; Macdiarmid, A. G., POLYANILINE, A NOVEL CONDUCTING POLYMER - MORPHOLOGY AND CHEMISTRY OF ITS OXIDATION AND REDUCTION IN AQUEOUS-ELECTROLYTES. *Journal of the Chemical Society-Faraday Transactions I* **1986**, *82*, 2385-&.
17. Prakash, R., Electrochemistry of polyaniline: Study of the pH effect and electrochromism. *Journal of Applied Polymer Science* **2002**, *83* (2), 378-385.
18. MacDiarmid, A. G. High Capacity Polyaniline Electrodes. 1990.
19. Cui, G.; Lee, J. S.; Kim, S. J.; Nam, H.; Cha, G. S.; Kim, H. D., Potentiometric pCO<sub>2</sub> sensor using polyaniline-coated pH-sensitive electrodes. *Analyst* **1998**, *123* (9), 1855-1859.
20. (a) Du, Z.; Li, C.; Li, L.; Yu, H.; Wang, Y.; Wang, T., Ammonia gas detection based on polyaniline nanofibers coated on interdigitated array electrodes. *Journal of Materials Science-Materials in Electronics* **2011**, *22* (4), 418-421;  
  
(b) Ansari, M. O.; Mohammad, F., Thermal stability, electrical conductivity and ammonia sensing studies on p-toluenesulfonic acid doped polyaniline:titanium dioxide (pTSA/Pani:TiO<sub>2</sub>) nanocomposites. *Sensors and Actuators B-Chemical* **2011**, *157* (1), 122-129.
21. Srivastava, S.; Kumar, S.; Singh, V. N.; Singh, M.; Vijay, Y. K., Synthesis and characterization of TiO<sub>2</sub> doped polyaniline composites for hydrogen gas sensing. *International Journal of Hydrogen Energy* **2011**, *36* (10), 6343-6355.
22. Hosseini, S. H.; Oskooei, S. H. A.; Entezami, A. A., Toxic gas and vapour detection by polyaniline gas sensors. *Iranian Polymer Journal* **2005**, *14* (4), 333-344.

23. Park, K.-I.; Song, H.-M.; Kim, Y.; Mho, S.-I.; Cho, W. I.; Yeo, I.-H., Electrochemical preparation and characterization of V<sub>2</sub>O<sub>5</sub>/polyaniline composite film cathodes for Li battery. *Electrochimica Acta: Republic of Korea*, 2010; Vol. 55, pp 8023-8029.
24. Prakash, R.; Santhanam, K. S. V., Electrochromic window based on polyaniline. *Journal of Solid State Electrochemistry* **1998**, 2 (2), 123-125.
25. Stejskal, J.; Gilbert, R. G., Polyaniline. Preparation of a conducting polymer (IUPAC technical report). *Pure and Applied Chemistry* **2002**, 74 (5), 857-867.
26. Wei, Y.; Jang, G.-W.; Chan, C.-C.; Hsueh, K. F., Polymerization of Aniline and Alkyl Ring-Substituted Anilines in the Presence of Aromatic Additives. *Journal of Physical Chemistry* **1990**, 94 (19).
27. Wang, Y. D.; Rubner, M. F., AN INVESTIGATION OF THE CONDUCTIVITY STABILITY OF ACID-DOPED POLYANILINES. *Synthetic Metals* **1992**, 47 (3), 255-266.
28. Maeda, Y.; Katsuta, A.; Nagasaki, K.; Kamiyama, M., ELECTROCHEMICAL AND THERMAL-BEHAVIOR OF POLYANILINE IN AQUEOUS-SOLUTION CONTAINING SO<sub>4</sub><sup>2-</sup> IONS. *Journal of the Electrochemical Society* **1995**, 142 (7), 2261-2265.
29. Heera, T. R.; Cindrella, L., PbS/CoS-PANI composite semiconductor films. *Materials Science in Semiconductor Processing* **2011**, 14 (2), 151-156.
30. Kulkarni, V. G., Polyanilines-progress in processing and applications. *Abstracts of Papers of the American Chemical Society* **1998**, 215, U424-U424.
31. Kittel, C., *Introduction to Solid State Physics*. 6th ed.; John Wiley & Sons Inc.: Chichester, New York, 1986.
32. Yakuphanoglu, F.; Senkal, B. F., Electronic and thermoelectric properties of polyaniline organic semiconductor and electrical characterization of Al/PANI MIS diode. *Journal of Physical Chemistry C* **2007**, 111 (4), 1840-1846.
33. Kiattibutr, P.; Tarachiwin, L.; Ruangchuay, L.; Sirivat, A.; Schwank, J., Electrical conductivity responses of polyaniline films to SO<sub>2</sub>-N<sub>2</sub> mixtures: effect of dopant type and doping level. *Reactive & Functional Polymers* **2002**, 53 (1), 29-37.
34. MacDiarmid, A. G., Synthetic metals: a novel role for organic polymers. *Synthetic Metals* **2001**, 125 (1), 11-22.

35. Daifuku, H.; Kawagoe, T.; Yamamoto, N.; Ohsaka, T.; Oyama, N., A STUDY OF THE REDOX REACTION-MECHANISMS OF POLYANILINE USING A QUARTZ CRYSTAL MICROBALANCE. *Journal of Electroanalytical Chemistry* **1989**, 274 (1-2), 313-318.
36. Macdiarmid, A. G.; Somasiri, N. L. D.; Mu, S. L.; Wu, W. Q.; Chiang, J. C.; Huang, W. S.; Halpern, M., POLYANILINE - A CATHODE-ACTIVE MATERIAL FOR RECHARGEABLE AQUEOUS BATTERIES. *Journal of the Electrochemical Society* **1984**, 131 (8), C328-C328.
37. Seymour, R. B., *Conducting Polymers*. Plenum: New York, 1981.
38. Li, P.; Tan, T. C.; Lee, J. Y., Corrosion protection of mild steel by electroactive polyaniline coatings. *Synthetic Metals* **1997**, 88 (3), 237-242.
39. Mailherandolph, C.; Desilvestro, J., MORPHOLOGY OF ELECTROPOLYMERIZED ANILINE FILMS MODIFIED BY PARAPHENYLENEDIAMINE. *Journal of Electroanalytical Chemistry* **1989**, 262 (1-2), 289-295.
40. Cooper, H.; Segal, E.; Srebnik, S.; Tchoudakov, R.; Narkis, M.; Siegmann, A., Electrically conductive sensors for liquids based on ternary immiscible polymer blends containing polyaniline. *Polymers for Advanced Technologies* **2004**, 15 (10), 573-582.
41. Knoll, M., Aufladepotential und Sekundäremission elektronenbestrahlter Körper. *Zeitschrift für technische Physik* **1935**, 16, 467-475.
42. Everhart, T. E., Persistence pays off: Sir Charles Oatley and the scanning electron microscope. *Journal of Vacuum Science & Technology B: Microelectronics and Nanometer Structures* **1996**, 14 (6), 3620.
43. Everhart, T. E.; Thornley, R. F. M., Wide-band detector for micro-microampere low-energy electron current. *Journal of Scientific Instruments* **1960**, 37 (7), 246-248.
44. Kubelka, P.; Munk, E., *Technical Physics* **1931**, 12, 593.
45. Skoog, D. A.; Holler, F. J.; Crouch, S. R., *Instrumental Analysis*. International ed.; Brooks/Cole: 2007.

46. Activated Platinum Surfaces: ELECTROCHEMICAL STUDIES OF TREATED ELECTRODES. *Platinum Metals Review* **1964**, 8 (4), 141-142.
47. Carrai, P.; Nucci, L.; Pergola, F., POLAROGRAPHIC-BEHAVIOR OF ALACHLOR APPLICATION TO ANALYTICAL DETERMINATION. *Analytical Letters* **1992**, 25 (1), 163-172.
48. Britton, H., *Hydrogen Ions*. 4th ed.; Chapman and Hall: London, 1952.
49. El-Shahawi, M. S.; Hamza, A.; Bashammakh, A. S.; Al-Sibaai, A. A.; Al-Saggaf, W. T., Analysis of Some Selected Persistent Organic Chlorinated Pesticides in Marine Water and Food Stuffs by Differential Pulse-Cathodic Stripping Voltammetry. *Electroanalysis* **2011**, 23 (5), 1175-1185.
50. Jensen, B. L., *ORGANIC CHEMISTRY LABORATORY MANUAL: CHY 254*. Department of Chemistry: University of Maine, 2011.
51. FTIR spectra of Alachlor.  
<http://webbook.nist.gov/cgi/cbook.cgi?Spec=C15972608&Index=0&Type=IR&Large=on>.
52. Agreda, V. H., *Acetic Acid and Its Derivatives*. New York, 1993.
53. Smith, J. G., *ORGANIC CHEMISTRY*. 2nd ed.; McGraw-Hill: 2008; p 960.

## **AUTHORS BIOGRAPHY**

Todd M. Conner was born on July 21, 1990 in Bryn Mawr, Pennsylvania. His family moved to Camden, Maine shortly after this. Todd spent the remainder of his childhood growing up in Camden and attended Camden Hills Regional High School. After graduating there in 2008 as a member of the Fellowship of Christian Athletes and the National Honor Society, he attended the University of Maine and studied in the Honors College, majoring in Chemistry. After graduating from the University of Maine cum laude in 2012, he will be attending graduate school at some point to further his education. Todd is a confirmed Anglican and loves Jesus; enjoys the outdoors through hiking, biking, and running; and plays many musical instruments including the guitar and the African drum, Djembe.